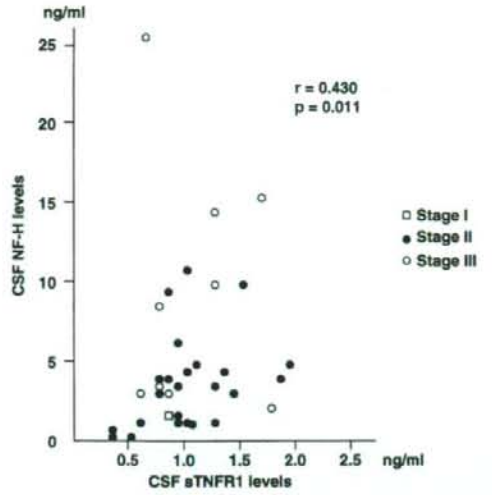

Fig. 4. Relationship between CSF NF-H and sTNFR1 levels in SSPE patients. r, Spearman's coefficient.

0.54, 0.63, and 0.91 ng/ml, respectively. He is still alive with coma and severe spastic tetraplegia 5 years after the onset.

4. Discussion

The prognosis of SSPE is still quite poor and most patients have a progressive course, resulting in a vegetative state or death within a few years from onset, although early diagnosis and treatment with interferon-α and ribavirin have improved the outcome to some extent (Hara et al., 2003; Solomon et al., 2002; Tomoda et al., 2001). Evaluation of disease progression and therapeutic effect has been based mainly on clinical symptoms, neurological findings including the neurological disability index score, brain imaging, anti-measles antibody titer, and quantified viral load (Dyken et al., 1982; Hara et al., 2003; Tomoda et al., 2001). However, a quantitative, chronological and convenient examination using a biomarker to indicate the degree of neurodegeneration during the clinical course of SSPE is unavailable.

Measurement of NF is useful to confirm neuronal injury (Osterlundh et al., 2008; Zachrisson et al., 2000; Zetterberg et al., 2006; Zetterberg et al., 2007a), to evaluate therapeutic effect (Abdulle et al., 2007; Mellgren et al., 2007; Tullberg et al., 2007), to predict prognosis (Nylén et al., 2006; Petzold et al., 2005, 2006; Rosén et al., 2004; Zetterberg et al., 2007a,b), and for differential diagnosis (Brettschneider et al., 2006). However, there are only a few reports of NF in pediatric disorders, including perinatal asphyxia and cerebral white matter abnormalities (Blennow et al., 2001; Kristjánsdóttir et al., 2001). Here, we provide the first report of CSF NF levels in SSPE. Our data show that these levels are significantly higher in SSPE patients than in age- and sex-matched controls, and higher in the later stage than in the earlier stage of the disease. We could entry only one SSPE patient in Jabbour stage I. Most of family of SSPE patients cannot think that they have any disease because symptoms are mild and slowly progressive in stage I, and it is hard to collect the samples from SSPE patients in stage I. In a 10-year-old Japanese boy with SSPE, CSF NF-H levels increased as his clinical condition and brain atrophy on MRI worsened. Therefore, an increase in CSF NF-H levels seems to reflect development of neuronal degeneration in SSPE.

Postmortem studies and brain biopsies have revealed expression of proinflammatory cytokines including TNF-α in brain lesions of SSPE (Anlar et al., 2001; Hofman et al., 1991; Nagano et al., 1994). Previous studies have shown that sTNFR is an inhibitor and natural homeostatic regulator of the action of TNF-α, and that its level, rather than that of TNF-α, reflects the true biological activity of TNF-α (Duncombe and Brenner, 1988; Engelmann et al., 1990; Seckinger et al., 1988). We have previously reported that CSF sTNFR1 levels were elevated in a boy with SSPE at 12 days before death (Ichiyama et al., 1997), and the present study showed that CSF sTNFR1 levels in SSPE patients were significantly higher than in controls. In addition, there was a significant correlation between CSF sTNFR1 and NF-H levels in SSPE patients. However, there was no significant difference in CSF sTNFR1 levels between SSPE patients in Jabbour stages II and III, and serial CSF sTNFR1 levels only showed small changes in the clinical course of the 10-year-old Japanese boy with SSPE. We have previously reported that CSF sTNFR1 levels are high in patients with acute encephalitis who died or had neurological sequelae, and these levels were higher than those in the SSPE patients in this study (Ichiyama et al., 1996a,b). The previous and present results in our studies indicate that TNF-α plays an important role in the neurodestructive pathogenesis of SSPE, including in acute changes for the worse.

In conclusion, both CSF NF-H and sTNFR1 levels are elevated in SSPE patients, and the CSF NF-H level may serve as a quantitative biomarker of neuronal degeneration and disease progression in SSPE.

Acknowledgments

This work was supported by grants from the Research on Measures for Intractable Diseases (Prion Disease and Slow Virus Infections) of the Ministry of Health, Labour and Welfare of Japan.

References

Abdulle, S., Mellgren, A., Brew, B.J., Cinque, P., Hagberg, L., Price, R.W., Rosengren, L., Gisslén, M., 2007. CSF neurofilament protein (NFL)—a marker of active HIV-related neurodegeneration. J. Neurol. 254, 1026–1032.
Anlar, B., Söylemezoğlu, F., Aysun, S., Köse, G., Belen, D., Yalaz, K., 2001. Tissue inflammatory response in subacute sclerosing panencephalitis (SSPE). J. Child Neurol. 16, 895–900.
Blennow, M., Sävman, K., Ilves, P., Thoresen, M., Rosengren, L., 2001. Brain-specific proteins in the cerebrospinal fluid of severely asphyxiated newborn infants. Acta Paediatr. 90, 1171–1175.
Brettschneider, J., Petzold, A., Süßmuth, S.D., Landwehrmeyer, G.B., Ludolph, A.C., Kassubek, J., Tumani, H., 2006. Neurofilament heavy-chain NfH (SMI35) in cerebrospinal fluid supports the differential diagnosis of Parkinsonian syndromes. Mov. Disord. 21, 2224–2227.
Duncombe, A.S., Brenner, M.K., 1988. Is circulating tumor necrosis factor bioactive? N. Engl. J. Med 319, 1227.
Dyken, P.R., Swift, A., DuRant, R.H., 1982. Long-term follow-up of patients with subacute sclerosing panencephalitis treated with inosiplex. Ann. Neurol. 11, 359–364.
Engelmann, H., Novick, D., Wallach, D., 1990. Two tumor necrosis factor-binding proteins purified from human urine; evidence for immunological cross-reactivity with cell surface tumor necrosis factor receptor. J. Biol. Chem. 265, 1531–1536.
Garg, R.K., 2002. Subacute sclerosing panencephalitis. Postgrad. Med. J. 78, 63–70.
Hara, S., Kimura, H., Hoshino, Y., Hayashi, N., Negoro, T., Okumura, A., Kajita, Y., Sakuma, T., Nakayama, T., Hosoya, M., Tomoda, A., Morisima, T., 2003. Combination therapy with intraventricular interferon-alpha and ribavirin for subacute sclerosing panencephalitis and monitoring measles virus RNA by quantitative PCR assay. Brain Dev. 25, 367–369.
Hofman, F.M., Hinton, D.R., Baemayr, J., Weil, M., Merrill, J.E., 1991. Lymphokines and immunoregulatory molecules in subacute sclerosing panencephalitis. Clin. Immunol. Immunopathol. 58, 331–342.
Ichiyama, T., Hayashi, T., Furukawa, S., 1996a. Cerebrospinal fluid concentrations of soluble tumor necrosis factor receptor in bacterial and aseptic meningitis. Neurology 46, 837–838.
Ichiyama, T., Hayashi, T., Nishikawa, M., Furukawa, S., 1996b. Cerebrospinal fluid levels of soluble tumor necrosis factor receptor in acute encephalitis. J. Neurol. 243, 457–460.
Ichiyama, T., Hayashi, T., Furukawa, S., 1997. Subacute sclerosing panencephalitis. Neurology 48, 1142–1143.
Ichiyama, T., Siba, P., Suarkia, D., Reeder, J., Takasu, T., Miki, K., Maeba, S., Furukawa, S., 2006. Analysis of serum and cerebrospinal fluid cytokine levels in subacute sclerosing panencephalitis in Papua New Guinea. Cytokine 33, 17–20.
Jabbour, J.T., Duenas, D.A., Modlin, J., 1975. SSPE: clinical staging, course and frequency. Arch. Neurol. 32, 493–494.
Kristjánsdóttir, R., Uvebrant, P., Rosengren, L., 2001. Glial fibrillary acidic protein and neurofilament in children with cerebral white matter abnormalities. Neuropediatrics 32, 307–312.

Lewis, S.B., Wolper, R.A., Miralia, L., Yang, C., Shaw, G., 2008. Detection of phosphorylated NF-H in the cerebrospinal fluid and blood of aneurismal subarachnoid hemorrhage patients. J. Cereb. Blood Metab. 28, 1261–1271.
Mellgren, A., Price, R.W., Hagberg, L., Rosengren, L., Brew, B.J., Gisslén, M., 2007. Antiretroviral treatment reduces increased CSF neurofilament protein (NFL) in HIV-1 infection. Neurology 69, 1536–1541.
Mustafa, M.M., Lebel, M.H., Ramilo, O., Olsen, K.D., Reisch, J.S., Beutler, B., McCracken Jr., G.H., 1989. Correlation of interleukin-1β and cachectin concentrations in cerebrospinal fluid and outcome from bacterial meningitis. J. Pediatr. 115, 208–213.
Nagano, I., Nakamura, S., Yoshioka, M., Onodera, J., Kogure, K., Itoyama, Y., 1994. Expression of cytokines in brain lesions in subacute sclerosing panencephalitis. Neurology 44, 710–715.
Nyl é n, K., Csajbok, L.Z., Öst, M., Rashid, A., Karlsson, J.E., Blennow, K., Nellgård, B., Rosengren, L., 2006. CSF-neurofilament correlates with outcome after aneurysmal subarachnoid hemorrhage. Neurosci. Lett. 404, 132–136.
Osterlundh, G., Kjellmer, I., Lannering, B., Rosengren, L., Nilsson, U.A., Márky, I., 2008. Neurochemical markers of brain damage in cerebrospinal fluid during induction treatment of acute lymphoblastic leukemia in children. Pediatr. Blood Cancer 50, 793–798.
Petzold, A., 2005. Neurofilament phosphoforms: surrogate markers for axonal injury, degeneration and loss. J. Neurol. Sci. 233, 183–198.
Petzold, A., Eikelenboom, M.J., Keir, G., Grant, D., Lazeron, R.H., Polman, C.H., Uitdehaag, B.M., Thompson, E.J., Giovannoni, G., 2005. Axonal damage accumulates in the progressive phase of multiple sclerosis: three year follow up study. J. Neurol. Psychiatr. 76, 206–211.
Petzold, A., Hinds, N., Murray, N.M., Hirsch, N.P., Grant, D., Keir, G., Thompson, E.J., Reilly, M.M., 2006. CSF neurofilament levels: a potential prognostic marker in Guillain–Barré syndrome. Neurology 67, 1071–1073.
Rosén, H., Karlsson, J.E., Rosengren, L., 2004. CSF levels of neurofilament is a valuable predictor of long-term outcome after cardiac arrest. J. Neurol. Sci. 221, 19–24.
Salmaj, K.W., Raine, C.S., 1988. Tumor necrosis factor mediates myelin and oligodendrocyte damage in vitro. Ann. Neurol. 23, 339–346.
Sato, N., Goto, T., Haranaka, K., Satomi, N., Nariuchi, H., Mano-Hirano, Y., Sawasaki, Y., 1986. Actions of tumor necrosis factor on cultured vascular endothelial cells: morphologic modulation, growth inhibition, and cytotoxicity. J. Natl. Cancer Inst. 76, 1113–1121.
Seckinger, P., Issaz, S., Dayer, J.M., 1988. A human inhibitor of tumor necrosis factor α. J. Exp. Med. 167, 1511–1516.
Shaw, G., Yang, C., Ellis, R., Anderson, K., Parker, Mickle, J., Scheff, S., Pike, B., Anderson, D.K., Howland, D.R., 2005. Hyperphosphorylated neurofilament NF-H is a serum biomarker of axonal injury. Biochem. Biophys. Res. Commun. 336, 1268–1277.
Solomon, T., Hart, C.A., Vinjamuri, S., Beeching, N.J., Malucci, C., Humphrey, P., 2002. Treatment of subacute sclerosing panencephalitis with interferon-alpha, ribavirin, and inosiplex. J. Child Neurol. 17, 703–705.
Tomoda, A., Shiraishi, S., Hosoya, M., Hamada, A., 2001. Combined treatment with interferon-alpha and ribavirin for subacute sclerosing panencephalitis. Pediatr. Neurol. 24, 54–59.
Tullberg, M., Blennow, K., Månsson, J.E., Fredman, P., Tisell, M., Wikkelsö, C., 2007. Ventricular cerebrospinal fluid neurofilament protein levels decrease in parallel with white matter pathology after shunt surgery in normal pressure hydrocephalus. Eur. J. Neurol. 14, 248–254.
Zachrisson, O.C., Balldin, J., Ekman, R., Naesh, O., Rosengren, L., Agren, H., Blennow, K., 2000. No evident neuronal damage after electroconvulsive therapy. Psychiatry Res. 96, 157–165.
Zetterberg, H., Hietala, M.A., Jonsson, M., Andreasen, N., Styrud, E., Karisson, I., Edman, A., Popa, C., Rasulzada, A., Wahlund, L.O., Mehta, P.D., Rosengren, L., Blennow, K., Wallin, A., 2006. Neurochemical aftermath of amateur boxing. Arch. Neurol. 63, 1277–1280.
Zetterberg, H., Jacobsson, J., Rosengren, L., Blennow, K., Andersen, P.M., 2007a. Cerebrospinal fluid neurofilament light levels in amyotrophic lateral sclerosis: impact of SOD1 genotype. Eur. J. Neurol. 14, 1329–1333.
Zetterberg, H., Jonsson, M., Rasulzada, A., Popa, C., Styrud, E., Hietala, M.A., Rosengren, L., Wallin, A., Blennow, K., 2007b. No neurochemical evidence for brain injury caused by heading in soccer. Br. J. Sports Med. 41, 574–577.

THE JOURNAL OF COMPARATIVE NEUROLOGY 510:641–654 (2008)

Serine Racemase Is Predominantly Localized in Neurons in Mouse Brain

KAZUSHI MIYA,[1,2] RAN INOUE,[1] YOSHIMI TAKATA,[1] MANABU ABE,[3] RIE NATSUME,[3] KENJI SAKIMURA,[3] KAZUHISA HONGOU,[2] TOSHIO MIYAWAKI,[2] AND HISASHI MORI[1]*

[1]Department of Molecular Neuroscience, Graduate School of Medicine and Pharmaceutical Sciences, University of Toyama, Toyama 930-0194, Japan
[2]Department of Pediatrics, Graduate School of Medicine and Pharmaceutical Sciences, University of Toyama, Toyama 930-0194, Japan
[3]Department of Cellular Neurobiology, Brain Research Institute, Niigata University, Niigata 951-8585, Japan

ABSTRACT

D-Serine is the endogenous ligand for the glycine binding site of the *N*-methyl-D-aspartate (NMDA)-type glutamate receptor (GluR) channel and is involved in the regulation of synaptic plasticity, neural network formation, and neurodegenerative disorders. D-Serine is synthesized from L-serine by serine racemase (SR), which was first reported to be localized in astrocytes. However, recently, SR mRNA and its protein have been detected in neurons. In this study, we examined the SR distribution in the brain during postnatal development and in cultured cells by using novel SR knockout mice as negative controls. We found that SR is predominantly localized in pyramidal neurons in the cerebral cortex and hippocampal CA1 region. Double immunofluorescence staining revealed that SR signals colocalized with those of the neuron-specific nuclear protein, but not with the astrocytic markers glial fibrillary acid protein and 3-phosphoglycerate dehydrogenase. In the striatum, we observed SR expression in γ-aminobutyric acid (GABA)ergic medium-spiny neurons. Furthermore, in the adult cerebellum, we detected weak but significant SR signals in GABAergic Purkinje cells. From these findings, we conclude that SR is expressed predominantly in many types of neuron in the brain and plays a key role in the regulation of brain functions under physiological and pathological conditions via the production of the neuromodulator D-serine. J. Comp. Neurol. 510:641–654, 2008. © 2008 Wiley-Liss, Inc.

Indexing terms: D-serine; NMDA receptor; knockout mouse; cerebral cortex; hippocampus

The amino acid D-serine is the ligand for the glycine binding site of the *N*-methyl-D-aspartate (NMDA)-type glutamate receptor (GluR) channel (Kleckner and Dingledine, 1988). The NMDA-type GluR channel plays key roles in synaptic plasticity, neural network formation during development, and neurodegenerative and psychiatric disorders (Bliss and Collingridge, 1993; Komuro and Rakic, 1993; Lancelot and Beal, 1998; Coyle et al., 2003; Wang and Zhang, 2005). In the mammalian brain, D-serine is present at a level sufficient for the activation of the NMDA receptor channel (Hashimoto et al., 1993) and is abundant in the forebrain regions where NMDA-type GluRs are concentrated (Schell et al., 1997). Reduction of D-serine by D-amino acid oxidase (DAAO) suppresses NMDA receptor responses (Mothet et al., 2000) and diminishes long-term potentiation in neurons of the hippocampus (Yang et al., 2003) and the hypothalamic supraoptic nucleus (Panatier et al., 2006). In a developing cerebellum, D-serine has been shown to be required for granule cell migration via NMDA receptor activation (Kim et al., 2005). Furthermore, the reduction of D-serine by DAAO suppresses

Grant sponsor: Ministry of Education, Culture, Sports, Science, and Technology of Japan; Grant numbers: 507-16047210 and 507-18053008 (to H. M. for Scientific Research on Priority Areas on "Elucidation of glia-neuron network mediated information processing systems").

The first two authors contributed equally to this work.

*Correspondence to: Hisashi Mori, Ph. D., Department of Molecular Neuroscience, Graduate School of Medicine and Pharmaceutical Sciences, University of Toyama, Toyama 930-0194, Japan.

E-mail: hmori@med.u-toyama.ac.jp

Received 21 November 2007; Revised 22 February 2008; Accepted 11 July 2008

DOI 10.1002/cne.21822

Published online August 12, 2008 in Wiley InterScience (www.interscience.wiley.com).

© 2008 WILEY-LISS, INC.

NMDA-induced neurotoxicity in cortical and hippocampal slices (Katsuki et al., 2004; Shleper et al., 2005). From these results, D-serine is considered to be an endogenous ligand for the NMDA receptor in the brain.

D-Serine synthesis from L-serine is catalyzed by serine racemase (SR) (Wolosker et al., 1999). On the basis of the localizations of SR and D-serine in astrocytes, the release of D-serine from astrocytes in response to GluR stimulation (Schell et al., 1995), and the neuroactive function of D-serine (Mothet et al., 2000), D-serine can be considered as a gliotransmitter (Wolosker et al., 2002). The expressions of SR and D-serine are regulated by inflammatory stimuli (Wu and Barger, 2004; Wu et al., 2004; Sasabe et al., 2007) and are affected by neuronal activity (Hashimoto et al., 2007). The SR activity is enhanced by its interaction with the GluR-interacting protein (Kim et al., 2005), the presence of Mg^{2+} and ATP (De Miranda et al., 2002), and Ca^{2+} binding (Cook et al., 2002). In contrast, the enzymatic activity is suppressed by amino acids (Dunlop and Neidle, 2005) and *S*-nitrosylation (Mustafa et al., 2007).

Considering the role of D-serine in brain functions, information on the localization of SR that catalyzes D-serine synthesis is very important. The pioneering work of Wolosker et al. (1999) showed the glial localization of SR in the brain. However, recently, an immunohistochemical study and an in situ hybridization study have revealed the localization of the SR protein (Kartvelishvily et al., 2006) and its mRNA (Yoshikawa et al., 2007) in neurons. In this study, we examined the SR distribution in the brain during postnatal development and in cultured cells by using novel serine racemase knockout (SR-KO) mice as negative controls, and we found that the SR protein is predominantly localized in neurons but not in glial cells in brain sections.

MATERIALS AND METHODS

Generation of SR-KO mice

Animal care and experimental protocols were approved by the Animal Experiment Committee of the University of Toyama (Authorization No. 2006-med-93) and were carried out in accordance with the Guidelines for the Care and Use of Laboratory Animals of the University of Toyama.

We obtained the mouse bacterial artificial chromosome (BAC) clone RP23-284D9 carrying the SR gene from the BACPAC Resources Center CHORI (Oakland, CA). Using the counter-selection BAC modification kit (Gene Bridges, Dresden, Germany), we inserted the Cre recombinase-progesterone receptor fusion (CrePR) gene (Tsujita et al., 1999) linked to the DNA fragment containing the pgk-1 promoter-driven neomycin phosphotransferase gene (pgk-neo) flanked by two Flp recognition target (frt) sites (Takeuchi et al., 2002) into the SR gene at the +1 position. (Nucleotide residues of the mouse BAC clone are numbered in the 5′ to 3′ direction, beginning with the A of ATG, the initiation site of translation in the SR gene, which refers to position +1, and the preceding residues are indicated by negative numbers.) The nucleotide sequence of the mouse genome was obtained from the National Center for Biotechnology Information (NCBI Map Viewer, *Mus musculus* Build 36.1). We cloned the modified BAC DNA fragment inserted with the CrePR and pgk-neo genes and containing the 4.7-kb upstream (−4684 to −1) to 4.8-kb downstream (+2 to +4828) sequences of the SR gene into pMC1DTApMA (Kitayama et al., 2001) to generate the targeting vector pTVSRCP.

We used the C57BL/6-derived ES cell line RENKA (Fukaya et al., 2006) for the gene targeting. The ES cells were cultured as described (Mishina and Sakimura, 2007). In brief, the ES cells were cultured on mitomycin C-treated neomycin-resistant fibroblasts in Dulbecco's modified Eagle's medium supplemented with 15% fetal calf serum, 90.7 μM nonessential amino acids, 1 mM L-glutamine, 100 μM 2-mercaptoethanol, and 1×10^3 U/ml leukemia inhibitory factor (Chemicon, Temecula, CA) at 37°C under humidified atmosphere containing 5% CO_2. The targeting vector was linearized by *Not*I digestion and electroporated into ES cells by using Gene Pulser Xcell (Bio-Rad, Hercules, CA). G-418 selection (150 μg/ml) was started 36–48 hours after electroporation and continued for 1 week. We identified a recombinant ES cell clone (no. 107) by Southern blot analysis, and the recombinant ES cells were injected into 8-cell-stage embryos of ICR mice. The embryos were cultured to blastocysts and transferred to the uterus of pseudopregnant ICR mice. The resulting chimeric mice were mated with C57BL/6 mice to establish the mutant mouse line.

For the screening of recombinant ES cell clones and gene-targeted mice by Southern blot analysis, the 5′ outer (−6716 to −5917) and 3′ outer (+4956 to +5741) probes amplified from the BAC clone, and the neo probe of the 0.6-kb *Pst*I fragment from pgk-neo were used. The polymerase chain reaction (PCR)-amplified DNA probes were verified by using the DNA sequencer PRISM 3100 (ABI).

In this study, we used SR-knockout (KO) and wild-type (WT) mice with a pure C57BL/6 genetic background. We defined the day after overnight mating as embryonic day 0 (E0), and the day of birth as postnatal day 1 (P1).

Northern blot analysis

Northern blot analysis was performed in accordance with the manufacturer's protocol by using the NorthernMax-Gly kit (Ambion, Austin, TX). In brief, total RNA samples prepared with TRIsol Reagent (Invitrogen, Carlsbad, CA) from the cerebral cortex of WT and SR-KO mice were separated by agarose gel electrophoresis and blotted on a positively charged membrane (Hybond N+, GE Healthcare, Buckinghamshire, UK). The membranes were hybridized with a ^{32}P-labeled SR cDNA fragment corresponding to exon 1 to 7 or a β-actin cDNA fragment corresponding to the protein-coding region.

Primary cell cultures

The WT and SR-KO mouse embryos at E16–18 were harvested by cesarean section from anesthetized pregnant mice. Hippocampi were isolated and digested in phosphate-buffered saline (PBS; pH 7.4) containing 0.25% trypsin for 20 minutes at 37°C. The supernatants were removed from the precipitated tissue samples. PBS containing 0.05% DNase and 1% trypsin inhibitor was added to the hippocampal tissues. The tissue samples were gently triturated with a fire-polished Pasteur pipette. Isolated cells were centrifuged at 200*g* for 5 minutes at 4°C. Cell pellets were gently resuspended in the culture medium described later, and 4×10^5 cells were seeded onto polyethyleneimine-coated glass coverslips in 35-mm culture dishes. The cells were plated in Neurobasal medium

TABLE 1. Primary Antibodies Used in the Present Study

Antibody	Immunogen	Host	Dilution	Source
Serine racemase monoclonal	Mouse serine racemase (a.a 127-246)	Mouse	1:100–1:2000	612052 BD Biosciences
Serine racemase polyclonal	Mouse serine racemase (a.a. 1-50)	Goat	1:100	sc-5751 Santa Cruz Biotechnology
GFAP monoclonal (clone G-A-5)	Purified GFAP from pig spinal cord	Mouse	1:300–1000	G3893 Sigma-Aldrich
NeuN monoclonal	Purified cell nuclei from mouse brain	Mouse	1:300	MAB377 Chemicon
Actin polyclonal	Human actin (a.a. 325-375)	Rabbit	1:4000	sc-1616-R Santa Cruz Biotechnology
MAP2 monoclonal	Purified rat brain microtubule MAP2	Mouse	1:500	05-334 Upstate Biotechnology
Parv polyclonal	Recombinant mouse parvalbumin (full length)	Goat	1:5000	M. Watanabe, Hokkaido University (Nakamura et al., 2004; Miura et al., 2006; Uchigashima et al., 2007)
VGluT1 polyclonal	Recombinant rat VGluT1 (a. a. 511-560)	Goat	1:500	M. Watanabe, Hokkaido University (Miyazaki et al., 2003; Miura et al., 2006; Uchigashima et al., 2007)
VGluT2 polyclonal	Recombinant rat VGluT2 (a. a. 519-582)	Goat	1:500	M. Watanabe, Hokkaido University (Miyazaki et al., 2003; Miura et al., 2006; Uchigashima et al., 2007)
3PGDH polyclonal	Recombinant rat 3PGDH (full length)	Rabbit	1:200	M. Watanabe, Hokkaido University (Yamasaki et al., 2001)
GAD polyclonal	Recombinant mouse GAD (a.a. 268-593)	Rabbit	1:200	M. Watanabe, Hokkaido University (Yamada et al., 2001; Uchigashima et al., 2007)

Abbreviations: a.a., amino acids; GAD, glutamic acid decarboxylase; GFAP, glial fibrillary acidic protein; MAP2, microtubule-associated protein 2; Parv, parvalbumin; 3PGDH, 3-phosphoglycerate dehydrogenase; VGluT, vesicular glutamate transporter.

(Invitrogen, Carlsbad, CA) supplemented with B27 (Invitrogen), 400 μM glutamine, and 5% fetal bovine serum. The medium was replaced every 5 days after seeding. Histochemical analysis was performed on days 5–10 of the culture period as described below.

Antibody characterization

Primary antibodies used in the present study are listed in Table 1. The mouse monoclonal anti-SR antibody was raised against amino acids 127–246 of mouse SR (BD Biosciences, San Jose, CA cat. no. 612052, lot no. 11719). This antibody detected a single band of ~38 kDa on a Western blot of brain homogenate from WT but not from SR-KO mice (Fig. 2). The goat polyclonal anti-SR antibody was raised against amino acids 1–50 of mouse SR (Santa Cruz Biotechnology, Santa Cruz, CA, cat. no. sc-5751, lot no. H2704). This antibody is reported to detect a single band of ~37 kDa on a Western blot (Puyal et al., 2006). No staining was observed when these anti-SR antibodies were used for immunostaining of brain sections from SR-KO mice (Figs. 3–7).

The mouse monoclonal anti-glial fibrillary acid protein (anti-GFAP) antibody was raised against purified GFAP from pig spinal cord (Sigma-Aldrich, St. Louis, MO, cat. no. G3893, clone G-A-5, lot no. 115k482). This antibody stained cells with the classic morphology and distribution of fibrillary astrocytes in our study.

The mouse monoclonal anti-neuron-specific nuclear protein (anti-NeuN) antibody was raised against purified cell nuclei from mouse brain (Chemicon, cat. no. MAB377, lot no. 0607036763). Immunostaining with this anti-NeuN antibody is reportedly observed in most neuronal cell types in the rodent nervous system, and the Western blot using this antibody shows three bands of approximately 46–48 kDa in brain homogenates (Mullen et al., 1992).

The rabbit polyclonal anti-actin antibody was raised against a peptide mapping at the C-terminus (amino acids 325–375) of actin of human origin (Santa Cruz Biotechnology, cat. no. sc-1616-R, lot no. 1105). This antibody stains a single band of 42 kDa on a Western blot.

The mouse monoclonal anti-microtubule-associated protein 2 (anti-MAP2) antibody was raised against the purified rat brain microtubule MAP2 (Upstate Biotechnology, Lake Placid, NY, cat. no. 05-334, lot no. 14004). This antibody showed selective labeling of dendrites in neuron in our study, as reported previously (Philpot et al., 1997; Eiraku et al., 2002; Rameau et al., 2004).

The goat polyclonal anti-parvalbumin (anti-Parv) antibody, the goat polyclonal anti-vesicular glutamate transporter 1 (anti-VGluT1) and anti-VGluT2 antibodies, the rabbit polyclonal anti-3-phosphoglycerate dehydrogenase (anti-3PGDH) antibody, and the rabbit polyclonal anti-glutamic acid decarboxylase (anti-GAD) antibody were kindly provided by Dr. Masahiko Watanabe (Hokkaido University, Japan).

The anti-Parv antibody was raised against a fusion protein of glutathione S-transferase (GST) and full length of mouse parvalbumin (amino acids 1–110). This antibody recognizes a single protein band at 13 kDa on a Western blot and selectively labels a subpopulation of GAD-positive inhibitory neurons (Nakamura et al., 2004; Miura et al., 2006; Uchigashima et al., 2007).

The anti-VGluT1 and anti-VGluT2 antibodies were raised against GST-fusion proteins containing amino acids 511–560 of rat VGluT1 and amino acids 519–582 of rat VGluT2, respectively. These antibodies stain a protein band at around 60 kDa in the adult mouse brain on an immunoblotting. The characteristic immunolabeling was abolished almost completely by use of the same antibodies preabsorbed with antigen proteins. VGluT1 and VGluT2 are expressed in glutamatergic neurons and concentrate in their nerve terminals (Miyazaki et al., 2003; Miura et al., 2006; Uchigashima et al., 2007).

The anti-3PGDH antibody was raised against a recombinant protein of full-length rat 3PGDH expressed in *E. coli*. This antibody recognizes a single protein band at 57 kDa on a Western blot. The immunohistochemical signals obtained with this antibody were abolished almost completely by use of the primary antibody preabsorbed with the antigen protein. 3PGDH is expressed exclusively in

astrocytes in the cerebral cortex and Bergmann glia cells in the cerebellum (Yamasaki et al., 2001).

The anti-GAD antibody was raised against the recombinant mouse GAD (amino acids 268–593) expressed in *E. coli*. This antibody stains a major band at 67 kDa and an additional weak band at 65 kDa on a Western blot and labels γ-aminobutyric acid (GABA)-synthesizing neurons (Yamada et al., 2001).

Western blotting

The mice at P7, P14, P21, P28, and P56 were deeply anesthetized with an overdose of pentobarbital sodium (100 mg/kg body weight, i.p.) and then perfused transcardially with PBS. The cerebral cortex, hippocampus, and cerebellum were dissected and frozen in liquid nitrogen. Brain tissue was homogenized in ice-cold Mammalian Tissue Extraction Reagent (Pierce, Rockford, IL). The homogenate was centrifuged at 15,000 rpm for 15 minutes to remove large debris. The protein concentration was determined by using the BCA Protein Assay kit (Pierce), and then the protein samples were diluted at 1:1 in sample buffer (50 mM Tris-HCl, pH 6.8, 2% sodium dodecyl sulfate [SDS], 10% glycerol, 6% 2-mercaptoethanol, and 0.01% bromophenol blue). After denaturation by heating at 95°C for 5 minutes, 30 μg of protein was fractionated by 10% SDS-polyacrylamide gel electrophoresis (SDS-PAGE) and electroblotted onto a polyvinylidene difluoride (PVDF) membrane (Perkin-Elmer Life Sciences, Boston, MA). After blocking with 5% skim milk in PBS containing 0.1% Tween-20, the membranes were incubated with the primary mouse monoclonal anti-SR antibody (1:500) or rabbit polyclonal anti-actin antibody (1:4,000) for 2 hours at room temperature and then with horseradish peroxidase (HRP)-conjugated secondary antibody (anti-mouse IgG, 1:4,000 or anti-rabbit IgG, 1:5,000; Santa Cruz Biotechnology and Bio-Rad) for 1 hour at room temperature. Protein bands were detected by using the ECL chemiluminescence detection system (GE Healthcare).

Immunohistochemistry of brain sections

The mice at P7, P14, P21, P28, and P56 were deeply anesthetized with an overdose of pentobarbital sodium (100 mg/kg body weight, i.p.), perfused transcardially with PBS, and then perfused with 0.1 M phosphate buffer (PB; pH 7.4) containing 4.0% (w/v) paraformaldehyde. The brains were removed and postfixed overnight at 4°C in the same fixative. After cryoprotection with 30% (w/v) sucrose in PB, the brains were cut into 10-μm-thick sections by using a freezing microtome.

For the double immunofluorescence staining, after blocking with Mouse Ig Blocking Reagent (Vector, Burlingame, CA) and Protein Block Serum-Free (DakoCytomation, Carpinteria, CA), the sections were incubated with primary antibodies (goat polyclonal anti-SR, 1:100; anti-Parv, 1:5,000; anti-VGluT1, 1:500; anti-VGluT2, 1:500; mouse monoclonal anti-SR, 1:100; anti-NeuN, 1:300; anti-GFAP, 1:300; rabbit polyclonal anti-3PGDH, 1:200; and anti-GAD, 1:200) overnight at room temperature. Then the sections were incubated with Alexa 488-, 568-, 594-, and Cy5-labeled species-specific secondary antibodies (Invitrogen, Carlsbad, CA) diluted at 1:500 for 1 hour at room temperature. Images were taken with a confocal laser scanning microscope Leica TCS-SP5 (Leica Microsystems, Mannheim, Germany) by using laser lines at 488 nm (Ar laser), 568/594 nm (Green Diode laser), and 633 nm (He/Ne laser).

For light microscopy immunoperoxidase detection, tissue sections were treated with distilled water containing 0.3% hydrogen peroxide and 0.1% NaN_3 for 10 minutes at room temperature and then rinsed in PBS. After blocking with Mouse Ig Blocking Reagent (Vector) and Protein Block Serum-Free (DakoCytomation), the sections were incubated with a mouse anti-SR monoclonal antibody (1:2,000) diluted in PBS containing 1.0% bovine serum albumin (BSA) overnight at 4°C. After PBS rinses, the sections were incubated in biotinylated goat anti-mouse IgG (1.5 μg/ml for P7 sections and 15 μg/ml for other ages; Vector) diluted in PBS containing 1.0% BSA for 1 hour, and then incubated with the avidin-biotin-peroxidase complex (Vector). After washing in PBS, the sections were briefly dipped in Tris buffer (50 mM; pH7.5) and incubated in Tris buffer containing 0.025% 3,3′-diaminobenzidine tetrahydrochloride (DAB) and 0.005% hydrogen peroxide for 10 minutes. The nuclei were counterstained with hematoxylin. The sections were examined by using an Olympus AX80 microscope (Olympus, Tokyo, Japan).

Immunocytochemistry of primary cultured cells

Cells on coverslips were rinsed in PBS and fixed with 4% paraformaldehyde in PB for 10 minutes at room temperature. After fixation, the cells were washed in PBS. Then they were incubated for 10 minutes in PBS containing 0.1% Triton X-100 for permeabilization and incubated in PBS containing 3.0% BSA for 30 minutes. Coverslips were incubated with primary antibodies (goat anti-SR antibody, 1:100; mouse anti-MAP2 antibody, 1:500; and mouse anti-GFAP, 1:1,000) overnight at 4°C, followed by

Fig. 1. Generation of serine racemase (SR) knockout mice with C57BL/6 genetic background. **A:** Schematic representation of SR cDNA, SR gene, targeting vector, and targeted gene. Coding and noncoding regions of SR cDNA and exons (2–9) are indicated with closed and open boxes, respectively. Met is the initiation site of translation in the SR gene. Inserted CrePR and pgk-neo genes are shown. Relevant restriction enzyme sites (*ApaI* and *SpeI*) and the location of probes used (5′ outer, neo, and 3′ outer) are indicated. BSK, plasmid pBluescript; DT, diphtheria toxin gene. **B:** Southern blot analysis of genomic DNA from $SR^{+/+}$ (+/+), $SR^{+/-}$ (+/−), and $SR^{-/-}$ (−/−) mice. Left, *Spe*I-digested DNA hybridized with the 5′ outer probe; middle, *Spe*I-digested DNA hybridized with the 3′ outer probe; right, *Apa*I-digested DNA hybridized with the neo probe. The positions of DNA size markers are indicated on the left side. This Southern blot and sequencing of targeted genomic DNA fragments amplified by PCR reveal that the targeting vector with deletion of 460 bp at the 3′ end of the homologous arm is inserted into the SR locus. **C:** Northern blot analysis of total RNA extracted from the cerebral cortex of $SR^{+/+}$ (+/+), $SR^{+/-}$ (+/-), and $SR^{-/-}$ (-/-) mice. Five micrograms (left) and 1 μg (right) of total RNA blotted on membranes were hybridized with SR (left) and β-actin (right) probes. The positions of RNA size markers are indicated on the left side. **D:** Expression of SR protein in brain. Forebrain homogenate from $SR^{+/+}$ (+/+), $SR^{+/-}$ (+/−), and $SR^{-/-}$ (−/−) mice were separated by SDS-PAGE and immunoblotted with anti-SR antibody (upper) and anti-actin antibody (lower). The positions of protein size markers are indicated on the right side. The SR protein band of ~38 kDa size is detected in the WT mice, decreases in intensity in heterozygous mutant mice, and is not detected in homozygous mutant mice.

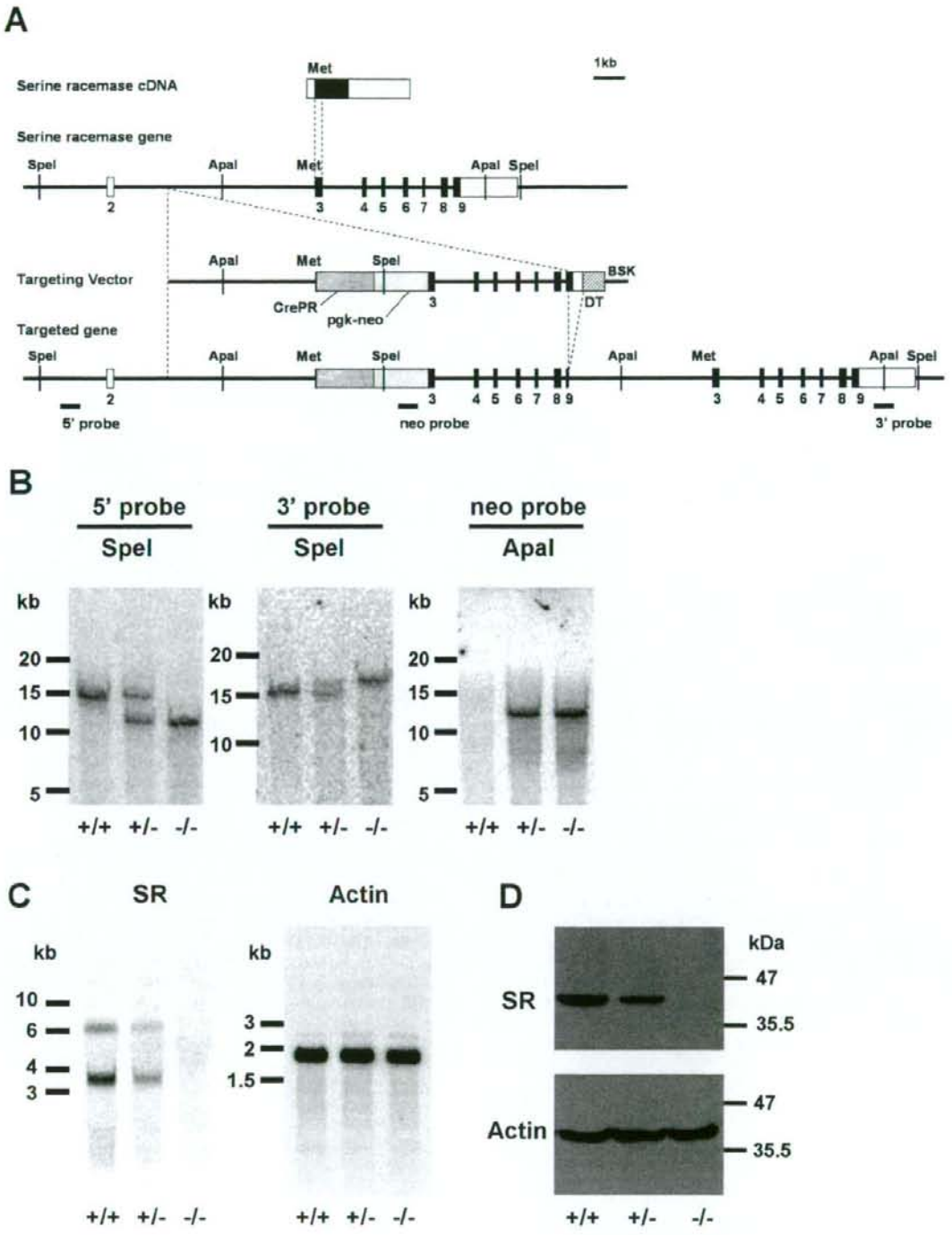
A
Serine racemase cDNA
Met
1kb
Serine racemase gene
SpeI
ApaI
Met
ApaI SpeI
2
3
4 5 6 7 8 9
Targeting Vector
ApaI
Met
SpeI
BSK
CrePR
pgk-neo
3
DT
Targeted gene
SpeI
ApaI
Met
SpeI
ApaI
Met
ApaI SpeI
2
3
4 5 6 7 8 9
3
4 5 6 7 8 9
5' probe
neo probe
3' probe
B
5' probe
SpeI
3' probe
SpeI
neo probe
ApaI
kb
20
15
10
5
+/+ +/- -/-
C
SR
Actin
kb
10
6
4
3
3
2
1.5
+/+ +/- -/-
D
kDa
SR
47
35.5
Actin
47
35.5
+/+ +/- -/-

Figure 1

an incubation with Alexa 488- and 568-labeled species-specific secondary antibodies (Invitrogen) diluted at 1:500 for 1 hour at room temperature. Images were taken with the confocal laser scanning microscope Leica TCS-SP5.

All the images were stored as TIFF files and processed by using Adobe Photoshop (San Jose, CA). The images were adjusted to optimize brightness, contrast, and sharpness and then assembled into figures. The red channel was then converted to magenta in Photoshop.

RESULTS

Generation of SR-KO mice

To disrupt the SR locus in ES cells derived from the C57BL/6 mouse strain, we constructed a targeting vector pTVSRCP in which the CrePR gene linked with the pgk-neo gene was inserted into the translation initiation site of the SR gene (Fig. 1A). We obtained one ES cell clone (no. 107) in which homologous recombination occurred at the SR locus as detected by using the 5′ outer probe. However, the sizes of the hybridizing bands with the 3′ outer and neo probes were inconsistent with the expected homologous recombination event. We performed further Southern blot analyses and sequencing of targeted genomic DNA fragments amplified by PCR, and revealed that the targeting vector with deletion of 460 bp at the 3′ end of the homologous arm was inserted into the SR locus (Fig. 1A). Chimeric mice derived from this ES clone were mated with C57BL/6 mice to establish the mutant mouse line (Fig. 1B). The expression of SR mRNA in the cerebral cortex was analyzed by Northern blotting. Major (3.6-kb) and minor (6.2-kb) bands were detected in the WT mice but not in the homozygous mutant mice (Fig. 1C). SR protein expression in the forebrain was examined by Western blot analysis. The SR protein band of ~38 kDa size was detected in the WT mice, whereas the SR protein signal was not detected in homozygous mutant mice (Fig 1D). These results indicate that the SR gene in the homozygous mutant mice was successfully disrupted by the insertional mutation of the targeting vector in the SR gene.

Although the detailed phenotypes of the SR-KO mice will be reported elsewhere (Inoue et al., in preparation), the SR-KO mice did not show any gross anatomical abnormality in the brain (see Fig. 3F).

Postnatal change in protein expression of serine racemase

We examined the SR protein level in the cortex and cerebellum during postnatal development by using Western blot analysis of mouse brain homogenate at P7, P14, P21, P28, and P56. The mouse anti-SR monoclonal antibody recognized a protein band of ~38 kDa corresponding to SR (Wolosker et al., 1999) in the WT cerebral cortex but not in the SR-KO cortex (Fig. 2A). The SR expression level increased gradually from P7 to P56 in the cortex (Fig. 2A). In the hippocampus, the SR expression level gradually increased from P7 to P56, similarly to that in the cortex (data not shown). In the cerebellum, the SR expression level was lower than that in the cortex; the signal intensity of SR increased transiently during P14 to P28 (Fig. 2B). These spatiotemporal expression patterns of the SR protein in the mouse brain are consistent with a previous report (Wang and Zhu, 2003). The SR protein was not detected in the cerebellum of SR-KO mice at any age.

Localization of serine racemase protein in brain during development

The overall distribution of SR in the brain during development was examined by immunohistochemistry by using the mouse anti-SR monoclonal antibody. In the WT mice, weak signals of SR immunopositivity were detected in the cortex and hippocampus at P7 (Fig. 3A). At P14 and P21, the SR immunostaining intensity increased and was detected in the cerebral cortex, hippocampus, olfactory bulb, olfactory tubercle, striatum, and substantia nigra pars reticulata (Figs. 3B,C). The signal intensity of SR immunopositivity increased further at P28 and P56 (Figs. 3D,E). In the brain of P56 mice, SR immunopositivity was predominantly localized to the forebrain regions such as the olfactory bulb, olfactory tubercle, cerebral cortex, hippocampus, and striatum. In the olfactory bulb, the SR immunopositivity was strong in the granular cell layer, and weak in the external and internal layers. In the cerebral cortex, the SR immunopositivity was strong in layers II/III and VI and was slightly weak in layers I and V. In the hippocampus, strong SR signals were detected in the pyramidal cell layer in CA1 and the granular cell layer in the dentate gyrus. The intensity of the immunopositivity signals was very weak in the lower brainstem except for the substantia nigra pars reticulata (Fig. 3E). Projection fibers from the striatum to the substantia nigra seemed to be SR-immunopositive as determined by careful examination (data not shown). Throughout postnatal development, the SR immunopositivity was predominant in the telencephalon at all ages and was very weak in the brainstem and cerebellum. Under the same conditions, the anti-SR antibody did not immunoreact with cells in any region of the adult SR-KO mice brain (Fig. 3F).

We further examined the SR staining pattern in detail in the brain of P56 WT mice. In the cerebral cortex, intense SR immunopositivity was predominantly detected in the cytoplasm of pyramidal neurons and shaft dendrites of layers II/III and VI. Some cells in the cerebral cortex were not SR-immunopositive (Fig. 4A). In the cerebellum, Purkinje cells and their dendrites showed weak immunoreactivity. The cells in the granular layer did not show any immunoreactivity (Fig. 4B). In the corpus callosum, low to moderate immunolabeling was detected in fiber bundles, but the signal was not detected in putative glial elements (Fig. 4C). In the SR-KO mice, the SR immunopositivity was not detected in these brain regions (Figs. 4D–F). In the hippocampal CA1 region, pyramidal cells had strong SR immunopositivity, and their apical dendrites extending from pyramidal cells to the stratum radiatum were also labeled (Fig. 4G). Granule cells in the dentate gyrus also showed high immunoreactivity (data not shown). In the striatum, many round cells presumed to be medium-spiny neurons showed intense SR immunopositivity (Fig. 4H). In the substantia nigra pars reticulata, there was fibrous SR immunopositivity in the neuropil, but the signal was absent in cell bodies (Fig. 4I). In the hypothalamic supraoptic nucleus (SON), although the nonspecific labeling was evident in the pia matter of the brain, the SR immnunopositivity was negligible (Figs. 4J,K).

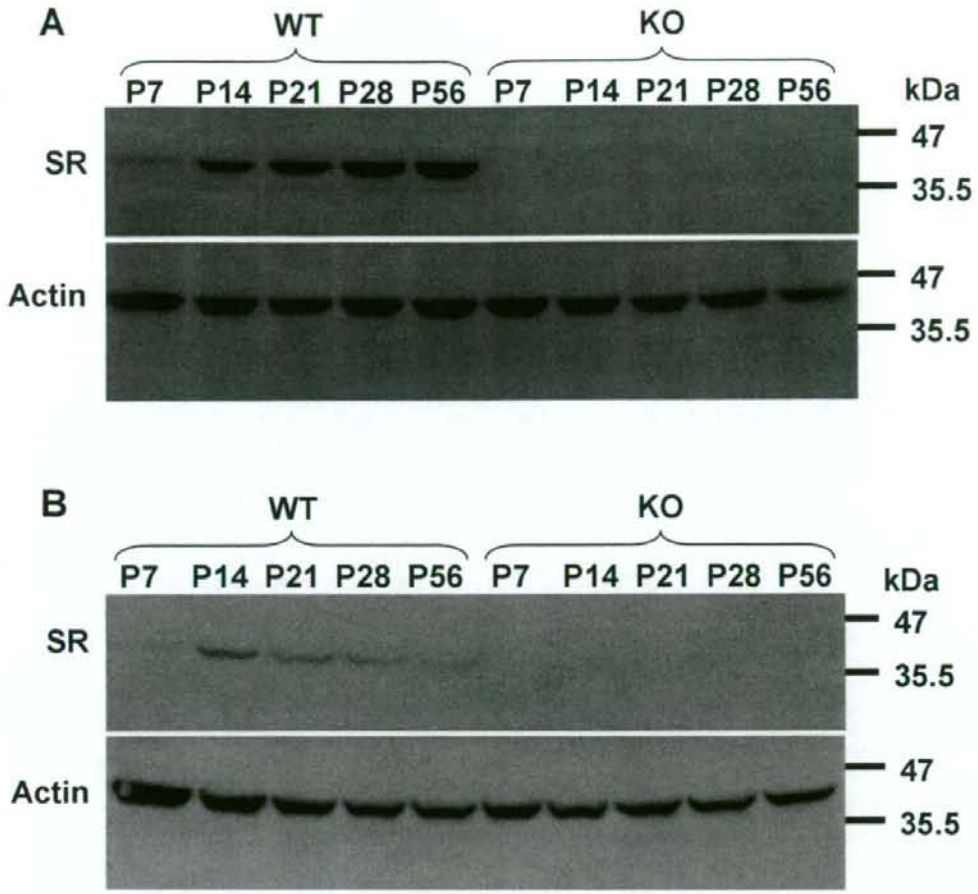

Fig. 2. Expression of serine racemase (SR) protein during postnatal development. **A,B:** Western blot analysis of cerebral cortex (A) and cerebellum (B) proteins of wild-type (WT) and SR knockout (KO) mice from postnatal day 7 (P7) to P56 using anti-SR antibody (upper panels of A and B) and anti-actin antibody (lower panels of A and B). The positions of protein size markers are indicated on the right side. The SR expression level increases gradually from P7 to P56 in the cortex and transiently increases in the cerebellum in WT mice. The SR band is not detected in SR-KO mice.

Identification of cells expressing serine racemase

We performed double immunofluorescence staining to identify the cell types expressing SR. SR immunopositivity was detected in the perikarya and colocalized with the neuronal marker NeuN protein in the cerebral cortex of WT P56 mice. There were some NeuN-positive but SR-negative cells in the cortex (Fig. 5A). In addition, no SR immunopositivity colocalized with the GABAergic neuronal marker proteins Parv and GAD (Figs. 5C,G). Furthermore, no SR immunoreactivity colocalized with the astrocytic marker proteins 3PGDH and GFAP in the cortex (Fig. 5E,F). No SR immunofluorescence was detected in the cortex of SR-KO mice (Fig. 5B,D). We were unable to detect SR in glutamate transporter VGluT1-labeled (Fig. 5H) or VGluT2-labeled (data not shown) glutamatergic terminals. Although the signals of immunofluorescence staining revealed by using the anti-SR polyclonal antibody (Figs. 5A,B) were slightly weaker than those of the anti-SR monoclonal antibody (Figs. 5C, D), the staining patterns were similar. From these results, we conclude that SR is expressed in glutamatergic neurons of the cerebral cortex and distributed preferentially in their somatodendritic elements.

In the adult cerebellum, weak SR immunopositivity was detected in Parv-labeled Purkinje cells of WT but not of SR-KO mice (Figs. 6A,B). No SR immunopositivity was detected in 3PGDH-positive Bergmann glia (Fig. 6C). In the corpus callosum, faint and granular SR immunopositivity was detected, but these SR signals showed no colocalization with GFAP signals (Fig. 6D). In the striatum, weak SR signals colocalized with the neural marker NeuN (Fig. 6E). SR and NeuN signals were detected in pyramidal cells of the hippocampus (Fig. 6F)

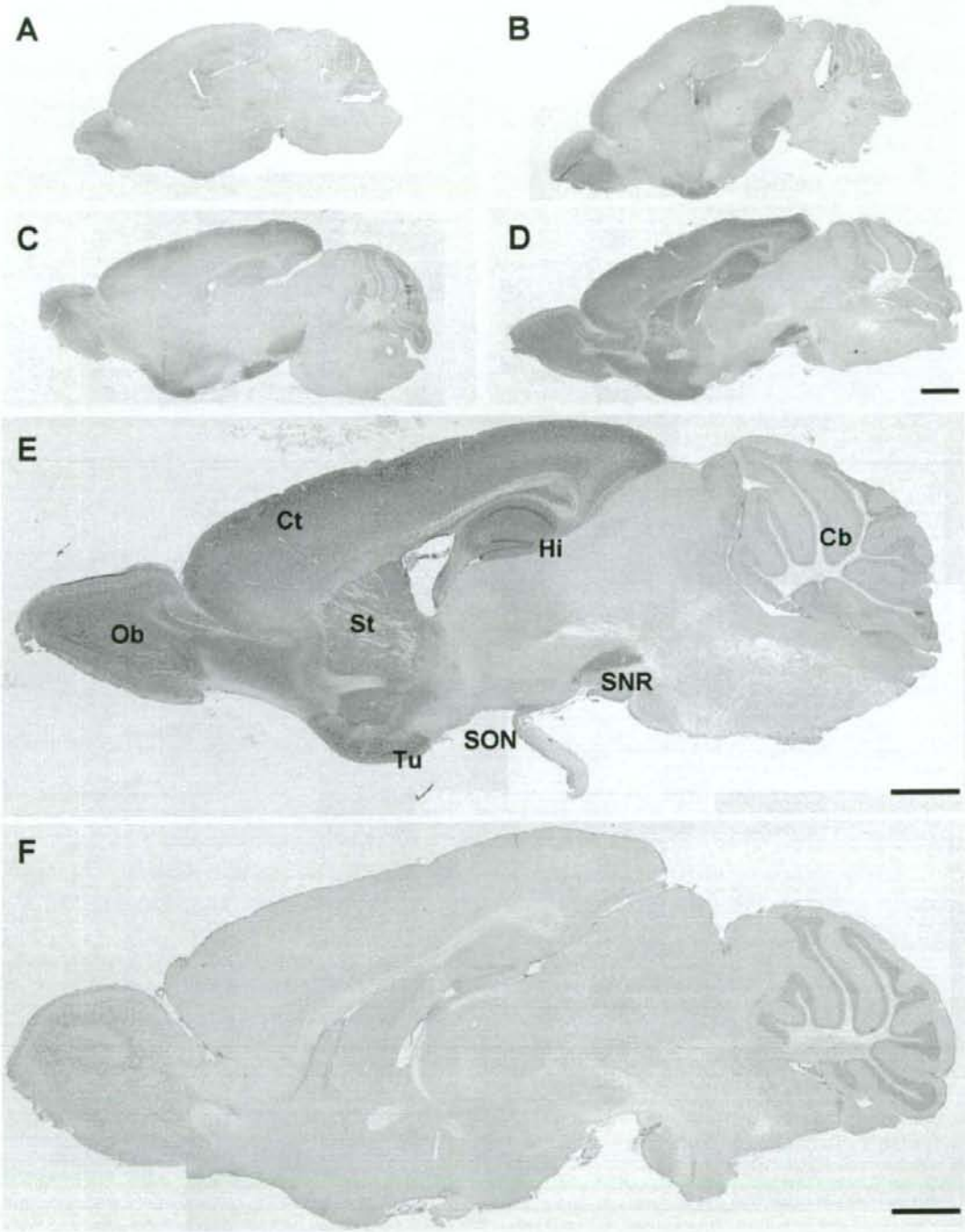

Fig. 3. Distribution of immunohistochemical staining of SR in mouse brain during postnatal development. **A–E:** Immunohistochemical staining of WT mice using anti-SR antibody at P7 (A), P14 (B), P21 (C), P28 (D), and P56 (E). **F:** Immunohistochemical staining of SR-KO mice using anti-SR antibody at P56. Abbreviations: Cb, cerebellum; Ct, cerebral cortex; Hi, hippocampus; Ob, olfactory bulb; SNR, substantia nigra pars reticulata; SON, supraoptic nucleus; St, striatum; Tu, olfactory tubercle. Throughout postnatal development, SR immunopositivity is predominant in the telencephalon at all ages and is very weak in the brainstem and cerebellum. Under the same conditions, the anti-SR antibody does not immunoreact with cells in any region of the SR-KO mice brain. Scale bar = 500 μm in D (applies to A–D); 1 mm in E,F.

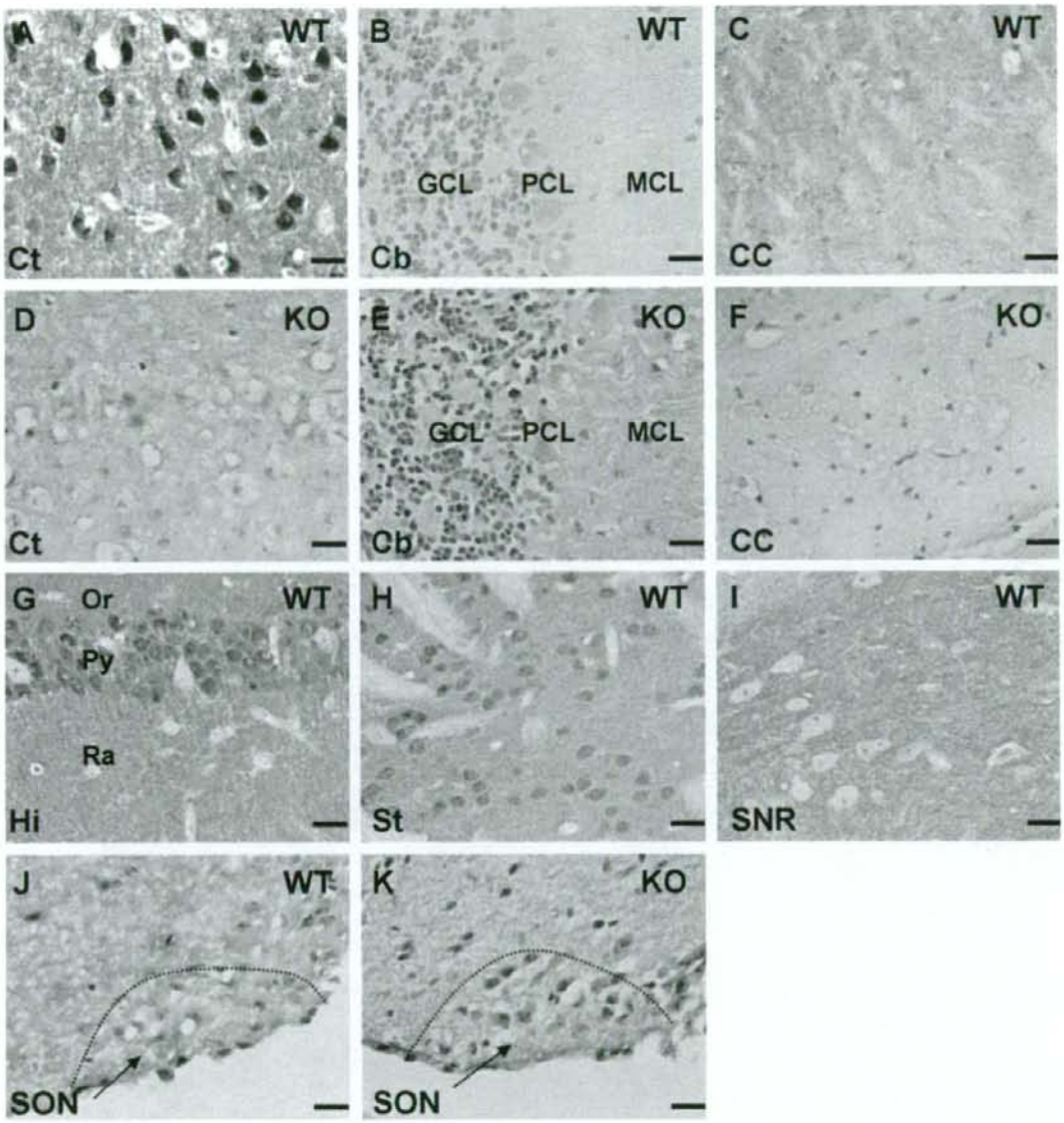

Fig. 4. Immunohistochemical staining patterns of SR in brain of P56 mice. **A–C, G–J:** Immunohistochemical staining of layers II–III of cerebral cortex (Ct, A), cerebellum (Cb, B), corpus callosum (CC, C), CA1 region of hippocampus (Hi, G), striatum (St, H), substantia nigra pars reticulata (SNR, I), and supraoptic nucleus (SON, J) of WT mice using anti-SR antibody. **D–F, K:** Immunohistochemical staining of layers II–III of cerebral cortex (Ct, D), cerebellum (Cb, E), corpus callosum (CC, F), and supraoptic nucleus (SON, K) of SR-KO mice using anti-SR antibody. Abbreviations: GCL, granule cell layer; MCL, molecular cell layer; Or, stratum oriens; PCL, Purkinje cell layer; Py, stratum pyramidale; Ra, stratum radiatum; SON, supraoptic nucleus. From these results, it can be seen that SR is expressed in principal neurons of given neural regions, irrespective of the excitatory or inhibitory signature. Scale bar = 20 μm in A–K.

and granule cells of the dentate gyrus (data not shown). However, no SR immunopositivity colocalized with the glial marker GFAP and GABAergic markers Parv and GAD (data not shown). Therefore, outside the cerebral cortex, SR is also expressed predominantly in neurons. In addition, SR immunopositivity was negligible and showed no colocalization with NeuN and GFAP in the SON (Figs. 6G,H).

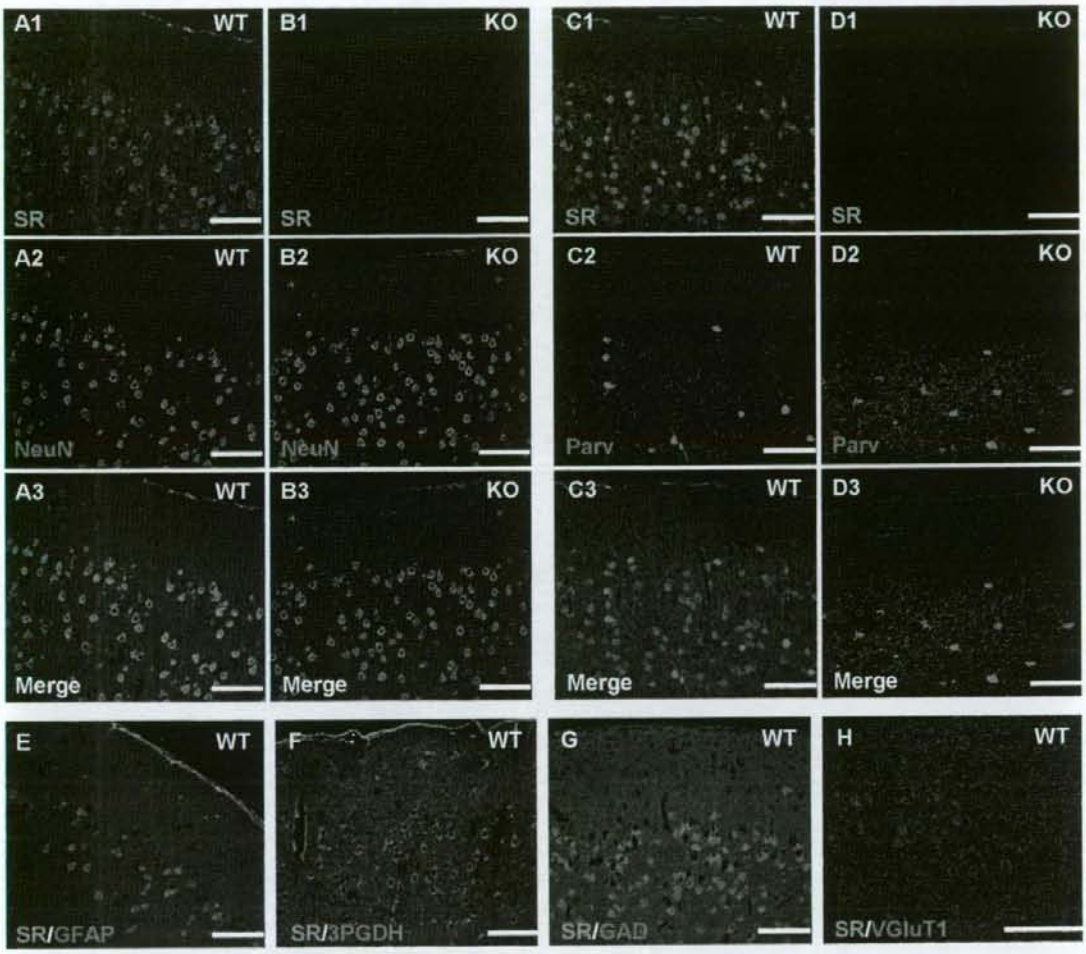

Fig. 5. Distribution of immunofluorescence staining pattern of SR in cerebral cortex of P56 mice. **A–D:** Double immunofluorescence staining analysis of cerebral cortex of WT (A,C) and SR-KO (B,D) mice at P56 using anti-SR antibody (SR, green, A1, A3, B1, B3, C1, C3, D1, and D3), anti-NeuN antibody (NeuN, magenta, A2, A3, B2, and B3), and anti-Parv antibody (Parv, magenta, C2, C3, D2, and D3). **E–H:** Double immunofluorescence staining of cerebral cortex of WT mice at P56 using anti-SR antibody (SR, green, E–H), anti-GFAP antibody (GFAP, magenta, E), anti-3PGDH antibody (3PGDH, magenta, F), anti-GAD antibody (GAD, magenta, G), and anti-VGluT1 antibody (VGluT1, magenta, H). Confocal micrographs of cerebral cortex sections double-labeled for known neuronal or glial markers (magenta) and SR (green) reveal neuronal localization of SR. Scale bar = 75 μm in A–H.

Expression of serine racemase in cultured cells

The SR expression is regulated under various conditions (Wu and Barger, 2004; Wu et al., 2004; Sasabe et al., 2007). We performed double immunofluorescence staining to examine the SR protein expression in primary cultured cells derived from mouse embryonic hippocampi. The SR signals were detected in MAP2-positive neuronal cells (Fig. 7A). Weak SR signals were also detected in MAP2-negative cells that seemed to be glial cells. SR was expressed in GFAP-positive astrocytes (Fig. 7C). From these results, we conclude that SR is expressed in both hippocampal primary cultured neurons and astrocytes. Under the same conditions, SR signals were absent in the cells derived from SR-KO mice (Figs. 7B,D).

DISCUSSION

In this study, we evaluated the specificity of immunohistochemical reactions by using the novel SR-KO mice as negative controls. We examined the SR distribution in the brain during postnatal development and in cultured cells, and we found that SR was predominantly localized in neurons but not in glial cells in the brain sections exam-

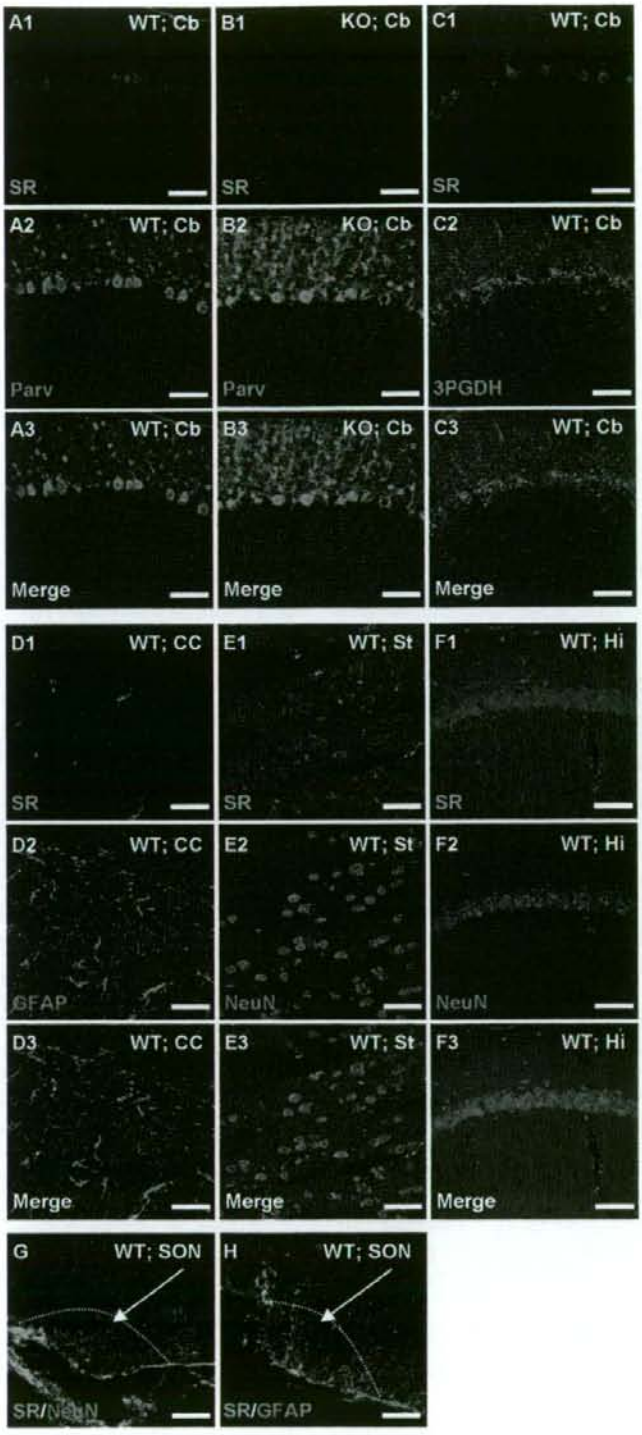

Fig. 6. Immunofluorescence localization of SR in brain of P56 mice. **A–C:** Double immunofluorescence staining of cerebellum (Cb, A–C) of WT (A,C) and SR-KO (B) mice using anti-SR antibody (SR, green, A1, A3, B1, B3, C1, and C3), anti-Parv antibody (Parv, magenta, A2, A3, B2, and B3), and anti-3PGDH antibody (3PGDH, magenta, C2 and C3). **D–F:** Double immunofluorescence staining of corpus callosum (CC, D), striatum (St, E), and hippocampus (Hi, F) of WT mice using anti-SR antibody (SR, green, D1, D3, E1, E3, F1, and F3), anti-GFAP antibody (GFAP, magenta, D2 and D3), and anti-NeuN antibody (NeuN, magenta, E2, E3, F2, and F3). **G,H:** Double immunofluorescence staining of supraoptic nucleus (SON) of WT mice using anti-SR antibody (SR, green, G,H), anti-NeuN antibody (NeuN, magenta, G), and anti-GFAP antibody (GFAP, magenta, H). Confocal micrographs of brain sections double-labeled for known neuronal or glial markers (magenta) and SR (green) reveal neuronal localization of SR. Scale bar = 75 μm in A–H.

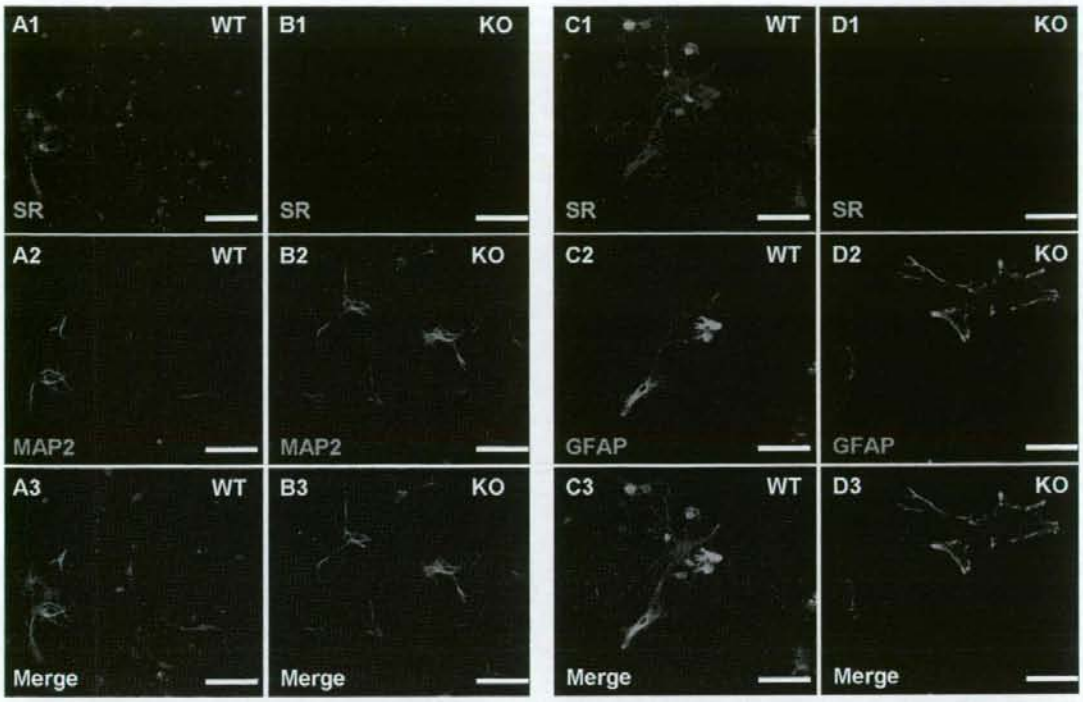

Fig. 7. Immunofluorescence localization of SR in cultured cells. **A–D:** Double immunofluorescence analysis of cultured cells derived from WT (A,C) and SR-KO (B,D) mice using anti-SR antibody (SR, green, A1, A3, B1, B3, C1, C3, D1, and D3), anti-MAP2 antibody (MAP2, magenta, A2, A3, B2, and B3), and anti-GFAP antibody (GFAP, magenta, C2, C3, D2, and D3). Confocal micrographs of cultured cells double-labeled for neuronal MAP2 (magenta) or glial GFAP (magenta) and SR (green) reveal both neuronal and glial localization of SR. Scale bar = 75 μm in A–D.

ined. Under the same conditions, no SR signals were detected in the brain by Western blot or immunohistochemical analyses in SR-KO mice. In contrast, SR signals were detected in both cultured neurons and astrocytes.

Detection of serine racemase in brain

In the pioneering work of Wolosker et al. (1999), they showed that SR is abundant in the glial cells of young (P13) rat brains. Subsequent studies using rhesus monkeys (Xia et al., 2004) and humans (Verrall et al., 2007) also showed the glial localization of SR in the brain. However, recent immunohistochemical staining of rat brain sections with new SR antibodies has revealed the significant neuronal as well as astrocytic staining of SR (Kartvelishvily et al., 2006). The predominant neuronal expression of SR mRNA has also been reported recently (Yoshikawa et al., 2007). We did not obtain evidence for glial localization of SR in the mouse brain, but we cannot exclude the possibility of a very low expression level of SR in glial cells in the brain. We used the anti-SR antibody at 1:100 dilution for double immunofluorescence staining. The use of a higher concentration of anti-SR antibody resulted in nonspecific staining in the brain sections of SR-KO mice (data not shown).

Thus, in our study, the immunofluorescence signals of SR are specific, but the sensitivity of the anti-SR antibody seems to be low. In the study of Wolosker et al. (1999), the antibody for immunohistochemical analysis was used only for freshly frozen sections fixed with methanol. They also reported that the immunopositivity for SR was absent in conventional aldehyde-fixed tissues. Thus, the immunohistochemical detection of SR depends on the antibodies used and the fixative conditions. We used the novel SR-KO mice as negative controls and detected the expression and localization of SR in neurons of the conventionally aldehyde-fixed brain from WT mice. Although it is possible that different animal species and different stages of development affect the immunohistochemical detection of SR, the distribution of SR should be clarified by using appropriate in vivo controls. Under culture conditions, SR is expressed in astrocytes, as reported previously (Wolosker et al., 1999; Panizzuti et al., 2001; Foltyn et al., 2005; Mothet et al., 2005) and as confirmed in this study (Fig. 7). The SR expression is regulated by extracellular signals such as inflammatory stimuli in vivo (Sasabe et al., 2007) and in vitro (Wu and Barger, 2004; Wu et al., 2004). Treatment of rats with the NMDA receptor antagonist MK-801 also affects SR mRNA expression (Hashimoto et al., 2007). Thus, it is still possible that experimental conditions of animals and cells affect the SR expression in the brain.

Neuronal localization of serine racemase in brain

There are no reports of detailed analysis of neurons expressing SR. Immunohistochemical analysis shows strong signals of SR immunopositivity in pyramidal neurons in the cerebral cortex (Fig. 4A). Double immunofluorescence staining also shows that the SR signals colocalize with the neuronal marker NeuN in the cerebral cortex. Furthermore, no SR signals colocalized with the GABAergic neuronal markers GAD and Parv nor with the astrocytic markers GFAP and 3PGDH (Fig. 5). From these results, we conclude that SR is localized in glutamatergic neurons in the cerebral cortex. In the hippocampus, we also detected strong signals of SR immunopositivity in glutamatergic pyramidal neurons. We detected the dendritic localization of SR signals in pyramidal neurons but not in VGluT1-labeled glutamatergic nerve terminals. Thus, SR is mainly present in the postsynaptic sites of these glutamatergic pyramidal neurons. Interestingly, it has been reported that neuronal activity inhibits SR activity by *S*-nitrosylation (Mustafa et al., 2007). In the striatum, we observed that the SR signals colocalized with NeuN in neurons. Because most neurons in the striatum are the GABAergic medium-spiny neurons (Kita and Kitai, 1988), we consider that SR is localized in GABAergic neurons (Fig. 4H). In the adult cerebellum, the SR expression level is lower than that in telencephalic regions. We detected weak but significant signals of SR in GABAergic Purkinje cells (Fig. 6). In situ hybridization analysis revealed the localization of SR mRNA in rat Purkinje cells (Yoshikawa et al., 2007). From these results, we conclude that SR is expressed in principal neurons of given neural regions, irrespective of the excitatory or inhibitory signature.

D-Serine synthesis from L-serine is catalyzed by SR, which is predominantly localized in neurons in the brain, as we have shown. The release of D-serine from neurons is regulated by neuronal activity, but the pathway for D-serine release is unknown (Kartvelishvily et al., 2006). D-Serine signaling is terminated by D-serine degradation by DAAO, which is expressed in the forebrain in humans (Verrall et al., 2007) and mainly in the cerebellum and brainstem in rats (Horiike et al., 1987; Schell et al., 1995). D-Serine can be removed from synaptic clefts by the amino acid transporter Asc-1 (Fukasawa et al., 2000), which is localized in the dendrites of neurons of the cerebral cortex (Matsuo et al., 2004). From our findings and these reports, we propose that D-serine is consistent with the definition of a neuron-derived neuromodulator.

Expression of serine racemase and brain functions

D-Serine is an important endogenous coagonist of the NMDA receptor channel, and its synthesis from L-serine is catalyzed by SR. The localization and regulation of SR expression are critical for the function of the NMDA receptor channel in the brain. Changes in D-serine and NMDA receptor activity are implicated in the pathophysiology of schizophrenia (Tsai et al., 1998; Olney et al., 1999). Increases in the SR expression level in the hippocampus (Steffek et al., 2006) and dorsolateral prefrontal cortex (Verrall et al., 2007) in schizophrenic patients were reported. However, SR immunopositivity is detected in glial cells (Verrall et al., 2007). SR expression is enhanced by the treatment of rats with the NMDA receptor antagonist MK-801 (Hashimoto et al., 2007). The antagonists of the NMDA receptor produce schizophrenic-like behavior in normal subjects (Javitt and Zukin, 1991; Coyle et al., 2003). Thus, it remains to be clarified whether the change in the SR expression level in schizophrenic patients is related to the cause or effect of the disease.

As mentioned, SR expression is upregulated in neurodegenerative amyotrophic lateral sclerosis (Sasabe et al., 2007). It is also important to examine SR expression during the course of development of other neurodegenerative diseases involving NMDA receptors such as focal ischemic brain injury, Parkinson's disease, Huntington's disease, and Alzheimer's disease (Lancelot and Beal, 1998). Our novel SR-KO mice will contribute to the analysis of the physiological and pathophysiological roles of SR and D-serine in vivo.

ACKNOWLEDGMENTS

We thank Prof. Masahiko Watanabe for providing many antibodies and critical reading of the manuscript, and Prof. Masakiyo Sasahara for the use of histochemical equipment and advice. We are grateful to Prof. Yoshihisa Kudo and Prof. Masayoshi Mishina for their encouragement and support.

LITERATURE CITED

Bliss TV, Collingridge GL. 1993. A synaptic model of memory: long-term potentiation in the hippocampus. Nature 361:31–39.

Cook SP, Galve-Roperh I, Martinez del Pozo A, Rodriguez-Crespo I. 2002. Direct calcium binding results in activation of brain serine racemase. J Biol Chem 277:27782–27792.

Coyle JT, Tsai G, Goff D. 2003. Converging evidence of NMDA receptor hypofunction in the pathophysiology of schizophrenia. Ann N Y Acad Sci 1003:318–327.

De Miranda J, Panizzutti R, Foltyn VN, Wolosker H. 2002. Cofactors of serine racemase that physiologically stimulate the synthesis of the *N*-methyl-D-aspartate (NMDA) receptor coagonist D-serine. Proc Natl Acad Sci U S A 99:14542–14547.

Dunlop DS, Neidle A. 2005. Regulation of serine racemase activity by amino acids. Brain Res Mol Brain Res 133:208–214.

Eiraku M, Hirata Y, Takeshima H, Hirano T, Kengaku M. 2002. Delta/notch-like epidermal growth factor (EGF)-related receptor, a novel EGF-like repeat-containing protein targeted to dendrites of developing and adult central nervous system neurons. J Biol Chem 277:25400–25407.

Foltyn VN, Bendikov I, De Miranda J, Panizzutti R, Dumin E, Shleper M, Li P, Toney MD, Kartvelishvily E, Wolosker H. 2005. Serine racemase modulates intracellular D-serine levels through an α,β-elimination activity. J Biol Chem 280:1754–1763.

Fukasawa Y, Segawa H, Kim JY, Chairoungdua A, Kim DK, Matsuo H, Cha SH, Endou H, Kanai Y. 2000. Identification and characterization of a Na(+)-independent neutral amino acid transporter that associates with the 4F2 heavy chain and exhibits substrate selectivity for small neutral D- and L-amino acids. J Biol Chem 275:9690–9698.

Fukaya M, Tsujita M, Yamazaki M, Kushiya E, Abe M, Akashi K, Natsume R, Kano M, Kamiya H, Watanabe M, Sakimura K. 2006. Abundant distribution of TARP γ-8 in synaptic and extrasynaptic surface of hippocampal neurons and its major role in AMPA receptor expression on spines and dendrites. Eur J Neurosci 24:2177–2190.

Hashimoto A, Nishikawa T, Oka T, Takahashi K. 1993. Endogenous D-serine in rat brain: *N*-methyl-D-aspartate receptor-related distribution and aging. J Neurochem 60:783–786.

Hashimoto A, Yoshikawa M, Andoh H, Yano H, Matsumoto H, Kawaguchi M, Oka T, Kobayashi H. 2007. Effects of MK-801 on the expression of serine racemase and d-amino acid oxidase mRNAs and on the D-serine levels in rat brain. Eur J Pharmacol 555:17–22.

Horiike K, Tojo H, Arai R, Yamano T, Nozaki M, Maeda T. 1987. Local-

ization of D-amino acid oxidase in Bergmann glial cells and astrocytes of rat cerebellum. Brain Res Bull 19:587–596.

Javitt DC and Zukin, 1991. Recent advances in the phencyclidine model of schizophrenia. Am J Psychiatry 148:1301–1308.

Kartvelishvily E, Shleper M, Balan L, Dumin E, Wolosker H. 2006. Neuron-derived D-serine release provides a novel means to activate *N*-methyl-D-aspartate receptors. J Biol Chem 281:14151–14162.

Katsuki H, Nonaka M, Shirakawa H, Kume T, Akaike A. 2004. Endogenous D-serine is involved in induction of neuronal death by *N*-methyl-D-aspartate and simulated ischemia in rat cerebrocortical slices. J Pharmacol Exp Ther 311:836–844.

Kim PM, Aizawa H, Kim PS, Huang AS, Wickramasinghe SR, Kashani AH, Barrow RK, Huganir RL, Ghosh A, Snyder SH. 2005. Serine racemase: activation by glutamate neurotransmission via glutamate receptor interacting protein and mediation of neuronal migration. Proc Natl Acad Sci U S A 102:2105–2110.

Kita H, Kitai SH. 1988. Glutamate decarboxylase immunoreactive neurons in rat neostriatum: their morphological types and populations. Brain Res 447:346–352.

Kitayama K, Abe M, Kakizaki T, Honma D, Natsume R, Fukaya M, Watanabe M, Miyazaki J, Mishina M, Sakimura K. 2001. Purkinje cell-specific and inducible gene recombination system generated from C57BL/6 mouse ES cells. Biochem Biophys Res Commun 281:1134–1140.

Kleckner NW, Dingledine R. 1988. Requirement for glycine in activation of NMDA-receptors expressed in *Xenopus* oocytes. Science 241:835–837.

Komuro H, Rakic P. 1993. Modulation of neuronal migration by NMDA receptors. Science 260:95–97.

Lancelot E, Beal MF. 1998. Glutamate toxicity in chronic neurodegenerative disease. Prog Brain Res 116:331–347.

Matsuo H, Kanai Y, Tokunaga M, Nakata T, Chairoungdua A, Ishimine H, Tsukada S, Ooigawa H, Nawashiro H, Kobayashi Y, Fukuda J, Endou H. 2004. High affinity D- and L-serine transporter Asc-1: cloning and dendritic localization in the rat cerebral and cerebellar cortices. Neurosci Lett 358:123–126.

Mishina M, Sakimura K. 2007. Conditional gene targeting on the pure C57BL/6 genetic background. Neurosci Res 58:105–112.

Miura E, Fukaya M, Sato T, Sugihara K, Asano M, Yoshioka K, Watanabe M. 2006. Expression and distribution of JNK/SAPK-associated scaffold protein JSAP1 in developing and adult mouse brain. J Neurochem 97:1431–1446.

Miyazaki T, Fukaya M, Shimizu H, Watanabe M. 2003. Subtype switching of vesicular glutamate transporters at parallel fibre-Purkinje cell synapses in developing mouse cerebellum. Eur J Neurosci 17:2563–2572.

Mothet JP, Parent AT, Wolosker H, Brady RO, Jr., Linden DJ, Ferris CD, Rogawski MA, Snyder SH. 2000. D-Serine is an endogenous ligand for the glycine site of the *N*-methyl-D-aspartate receptor. Proc Natl Acad Sci U S A 97:4926–4931.

Mothet JP, Pollegioni L, Ouanounou G, Martineau M, Fossier P, Baux G. 2005. Glutamate receptor activation triggers a calcium-dependent and SNARE protein-dependent release of the gliotransmitter D-serine. Proc Natl Acad Sci U S A 102:5606–5611.

Mullen RJ, Buck CR, Smith AM. 1992. NeuN, a neuronal specific nuclear protein in vertebrates. Development 116:201–211.

Mustafa AK, Kumar M, Selvakumar B, Ho GP, Ehmsen JT, Barrow RK, Amzel LM, Snyder SH. 2007. Nitric oxide S-nitrosylates serine racemase, mediating feedback inhibition of D-serine formation. Proc Natl Acad Sci U S A 104:2950–2955.

Nakamura M, Sato K, Fukaya M, Araishi K, Aiba A, Kano M, Watanabe M. 2004. Signaling complex formation of phospholipase Cβ4 with metabotropic glutamate receptor type 1α and 1,4,5-trisphosphate receptor at the perisynapse and endoplasmic reticulum in the mouse brain. Eur J Neurosci 20:2929–2944.

Olney JW, Newcomer JW, Farber NB. 1999. NMDA receptor hypofunction model of schizophrenia. J Psychiatr Res 33:523–533.

Panatier A, Theodosis DT, Mothet JP, Touquet B, Pollegioni L, Poulain DA, Oliet SH. 2006. Glia-derived D-serine controls NMDA receptor activity and synaptic memory. Cell 125:775–784.

Panizzutti R, De Miranda J, Ribeiro CS, Engelender S, Wolosker H. 2001. A new strategy to decrease *N*-methyl-D-aspartate (NMDA) receptor coactivation: inhibition of D-serine synthesis by converting serine racemase into an eliminase. Proc Natl Acad Sci U S A 98:5294–5299.

Philpot BD, Lim JH, Halpain S, Brunjes PC. 1997. Experience-dependent modifications in MAP2 phosphorylation in rat olfactory bulb. J Neurosci 17: 9596–9604.

Puyal J, Martineau M, Mothet JP, Nicolas MT, Raymond J. 2006. Changes in D-serine levels and localization during postnatal development of the rat vestibular nuclei. J Comp Neurol. 497:610–621.

Rameau GA, Chiu LY, Ziff EB. 2004. Bidirectional regulation of neuronal nitric-oxide synthase phosphorylation at serine 847 by the *N*-methyl-D-aspartate receptor. J Biol Chem 279:14307–14314.

Sasabe J, Chiba T, Yamada M, Okamoto K, Nishimoto I, Matsuoka M, Aiso S. 2007. D-Serine is a key determinant of glutamate toxicity in amyotrophic lateral sclerosis. Embo J 26:4149–4159.

Schell MJ, Brady RO Jr, Molliver ME, Snyder SH. 1997. D-Serine as a neuromodulator: regional and developmental localizations in rat brain glia resemble NMDA receptors. J Neurosci 17:1604–1615.

Schell MJ, Molliver ME, Snyder SH. 1995. D-Serine, an endogenous synaptic modulator: localization to astrocytes and glutamate-stimulated release. Proc Natl Acad Sci U S A 92:3948–3952.

Shleper M, Kartvelishvily E, Wolosker H. 2005. D-Serine is the dominant endogenous coagonist for NMDA receptor neurotoxicity in organotypic hippocampal slices. J Neurosci 25:9413–9417.

Steffek AE, Haroutunian V, Meador-Woodruff JH. 2006. Serine racemase protein expression in cortex and hippocampus in schizophrenia. Neuroreport 31:1181–1185.

Takeuchi T, Nomura T, Tsujita M, Suzuki M, Fuse T, Mori H, Mishina M. 2002. Flp recombinase transgenic mice of C57BL/6 strain for conditional gene targeting. Biochem Biophys Res Commun 293:953–957.

Tsai G, Yang P, Chung LC, Lange N, Coyle JT. 1998. D-Serine added to antipsychotics for the treatment of schizophrenia. Biol Psychiatry 44: 1081–1089.

Tsujita M, Mori H, Watanabe M, Suzuki M, Miyazaki J, Mishina M. 1999. Cerebellar granule cell-specific and inducible expression of Cre recombinase in the mouse. J Neurosci 19:10318–10323.

Uchigashima M, Narushima M, Fukaya M, Katona I, Kano M, Watanabe M. 2007. Subcellular arrangement of molecules for 2-arachidonoylglycerol-mediated retrograde signaling and its physiological contribution to synaptic modulation in the striatum. J Neurosci 27:3663–3676.

Verrall L, Walker M, Rawlings N, Benzel I, Kew JN, Harrison PJ, Burnet PW. 2007. d-Amino acid oxidase and serine racemase in human brain: normal distribution and altered expression in schizophrenia. Eur J Neurosci 26:1657–1669.

Wang LZ, Zhu XZ. 2003. Spatiotemporal relationships among D-serine, serine racemase, and D-amino acid oxidase during mouse postnatal development. Acta Pharmacol Sin 24:965–974.

Wang R, Zhang D. 2005. Memantine prolongs survival in an amyotrophic lateral sclerosis mouse model. Eur J Neurosci 22:2376–2380.

Wolosker H, Blackshaw S, Snyder SH. 1999. Serine racemase: a glial enzyme synthesizing D-serine to regulate glutamate-*N*-methyl-D-aspartate neurotransmission. Proc Natl Acad Sci U S A 96:13409–13414.

Wolosker H, Panizzutti R, De Miranda J. 2002. Neurobiology through the looking-glass: D-serine as a new glial-derived transmitter. Neurochem Int 41:327–332.

Wu S, Barger SW. 2004. Induction of serine racemase by inflammatory stimuli is dependent on AP-1. Ann N Y Acad Sci 1035:133–146.

Wu SZ, Bodles AM, Porter MM, Griffin WS, Basile AS, Barger SW. 2004. Induction of serine racemase expression and D-serine release from microglia by amyloid beta-peptide. J Neuroinflammation 1:2.

Xia M, Liu Y, Figueroa DJ, Chiu CS, Wei N, Lawlor AM, Lu P, Sur C, Koblan KS, Connolly TM. 2004. Characterization and localization of a human serine racemase. Brain Res Mol Brain Res 125:96–104.

Yamada K, Fukaya M, Shimizu H, Sakimura K, Watanabe M. 2001. NMDA receptor subunits GluRε1, GluRε3 and GluRζ1 are enriched at the mossy fibre-granule cell synapse in the adult mouse cerebellum. Eur J Neurosci 13:2025–2036.

Yamasaki M, Yamada K, Furuya S, Mitoma J, Hirabayashi Y, Watanabe M. 2001. 3-Phosphoglycerate dehydrogenase, a key enzyme for l-serine biosynthesis, is preferentially expressed in the radial glia/astrocyte lineage and olfactory ensheathing glia in the mouse brain. J Neurosci 21:7691–7704.

Yang Y, Ge W, Chen Y, Zhang Z, Shen W, Wu C, Poo M, Duan S. 2003. Contribution of astrocytes to hippocampal long-term potentiation through release of D-serine. Proc Natl Acad Sci U S A 100:15194–15199.

Yoshikawa M, Takayasu N, Hashimoto A, Sato Y, Tamaki R, Tsukamoto H, Kobayashi H, Noda S. 2007. The serine racemase mRNA is predominantly expressed in rat brain neurons. Arch Histol Cytol 70:127–134.

Pediatr Transplantation 2008: 12: 588–592

Copyright © 2008 Blackwell Munksgaard

Pediatric Transplantation
DOI: 10.1111/j.1399-3046.2007.00873.x

Two cases of chronic active Epstein–Barr virus infection in which EBV-specific cytotoxic T lymphocyte was induced after allogeneic bone marrow transplantation

Miyamura T, Chayama K, Wada T, Yamaguchi K, Yamashita N, Ishida T, Washio K, Morishita N, Manki A, Oda M, Morishima T. Two cases of chronic active Epstein–Barr virus infection in which EBV-specific cytotoxic T lymphocyte was induced after allogeneic bone marrow transplantation.
Pediatr Transplantation 2008: 12: 588–592. © 2008 Blackwell Munksgaard

Abstract: CAEBV is a high mortality and morbidity disease with life-threatening complications. Nevertheless, the treatment regimens for CAEBV have not yet been established. Although some reports have described CAEBV therapy involving treatments such as antiviral drugs, immunomodulatory agents, and immunochemotherapy, none of these treatments have been demonstrated to be effective. The only treatment reported to be effective is allogeneic SCT. However, the complications of SCT are severe, so treatment results have been poor. Recently, immunotherapy has been devised, but this is still in the developmental stage. In this report, two cases of CAEBV in which allogeneic SCT was performed soon after diagnosis are reported. In both cases, a high EBV genome titer in the peripheral blood was detected at onset. After SCT, the EBV genome titer decreased as CTL activity gradually increased. This fact suggested that not only high-dose chemotherapy as a pre-conditioning treatment of SCT but also increased CTL activity which could eliminate virus-infected cells might be effective, although additional cases should be studied in order to establish effective treatments.

Takako Miyamura, Kousuke Chayama, Tomoaki Wada, Kazunari Yamaguchi, Nobuko Yamashita, Toshiaki Ishida, Kana Washio, Naoto Morishita, Akira Manki, Megumi Oda and Tsuneo Morishima

Department of Pediatrics, Okayama University Graduate School of Medicine and Dentistry, Okayama, Japan

Key words: chronic active Epstein–Barr virus infection – bone marrow transplantation – cytotoxic T lymphocyte

Takako Miyamura, Okayama University Graduate School of Medicine and Dentistry, 2-5-1 Shikata-Cho, Okayama 700-8558, Japan
Tel.: +81 86 235 7251
Fax: +81 86 221 4745
E-mail: miyamu@md.okayama-u.ac.jp

Accepted for publication 15 November 2007

EBV is a DNA virus of the herpes virus family that asymptomatically infects most adults and persists for their lifetime (1, 2). Primary EBV infection is usually asymptomatic in childhood, but may induce acute infectious mononucleosis that resolves spontaneously. The virus carriers do not manifest symptoms as long as they are immunocompetent.

Abbreviations: BMT, bone marrow transplantation; CAEBV, chronic active Epstein–Barr virus infection; CPM, cyclophosphamide; CTL, cytotoxic T lymphocyte; EBV, Epstein–Barr virus; GVHD, graft-versus-host disease; LDH, lactose dehydrogenase; MTX, methotrexate; NK, natural killer; PCR, polymerase chain reaction; SCT, stem cell transplantation; STR, short tandem repeat; TBI, total body irradiation.

CAEBV is a heterogeneous EBV-related disorder characterized by chronic or recurrent infectious mononucleosis-like symptoms, such as lymphadenopathy, fever, hepatosplenomegaly, and pancytopenia, persisting for at least six months followed by hepatic, cardiac, or pulmonary dysfunction (3–6). The patients have very high viral copy numbers in their peripheral blood and abnormal antibody titers to EBV capsid antigen and early antigen. Although EBV usually infects B lymphocytes, in the case of CAEBV, either the T-cell or NK-cell compartments may also be involved (5–7).

The pathogenesis and etiology of CAEBV are not well characterized. Although the clonal expansion of EBV-associated T and NK cells has been suggested to play important roles in the pathogenesis of CAEBV (5, 6, 8, 9), it is

unclear whether CAEBV is truly a monoclonal disorder (10). It is not clear whether the EBV-associated abnormal cells cannot be excluded because of a factor on the virus side or a function on the host side. An effective therapy has not yet been developed. For patients with CAEBV, several treatments such as chemotherapy, antiviral drugs, steroids, and high-dose immunoglobulin have been tried, but only SCT has been reported to be effective (11–13). However, severe transplantation-related toxicity has occurred in most cases. Moreover, sometimes there is progressive deterioration even after aggressive chemotherapy or SCT.

We reported two CAEBV cases that underwent allogeneic SCT in their early clinical phase with successful results. We measured their viral copy numbers and CTL activity during their clinical courses. The viral copy numbers after SCT gradually decreased as the CTL activity improved.

Case reports

We reported two CAEBV cases that underwent allogeneic BMT in their early clinical phase with successful results. We diagnosed CAEBV based on the previous report (7), in which the following clinical features are commonly noted in patients with CAEBV. Symptoms are persistent and chronic and generally consist of prolonged or intermittent fever, lymphadenopathy, hepatosplenomegaly, fatigue, myalgia, and multiorgan failure.

Case 1

The patient was a five-yr-old boy who had exhibited prolonged fever, extensive lymphadenopathy, and severe liver dysfunction for more than six months. There was no family history of any similar disorders. Clonally proliferating EBV-infected T cells and abnormally high titers of EBV-related antibodies were detected. Fractionated CD4+ T cells contained a high EBV copy number (1.6×10^5 copies/μg DNA). EBV-terminal repeats showed a single band by Southern blotting analysis. NK-cell activity was normal. EBV-specific CTL activity was very low (0.02%, using the tetramer method). We diagnosed that the patient was suffering from CAEBV T-cell type, and he should receive SCT as soon as possible. Three months after diagnosis, the patient underwent allogeneic BMT from an HLA 1-locus mismatched donor: his mother.

The preconditioning regimen consisted of TBI, CPM, and thiotepa. Prophylaxis for GVHD consisted of cyclosporin A and short-term MTX. The donor had previously been infected with EBV. There were no severe complications of the BMT. Bone marrow recovery was steady and the neutrophil count was higher than 500/μL at day 15. Acute GVHD was grade 2 (intestine). The clinical course of the patient is depicted in Fig. 1. Symptoms such as the liver dysfunction, fever, and cervical lymph node swelling improved soon after high-dose chemotherapy had been started. Engraftment (46XX, 98% of BM cells) was obtained with no detectable EBV-DNA on day 28 after BMT. The EBV genome titer and EBV-specific CTL activity were measured during his clinical course, the former by real-time PCR (14) and the latter using the tetramer method (15). Before BMT, high EBV genome level was detected, while the CTL activity was very low (0.02%, using the tetramer method). After BMT,

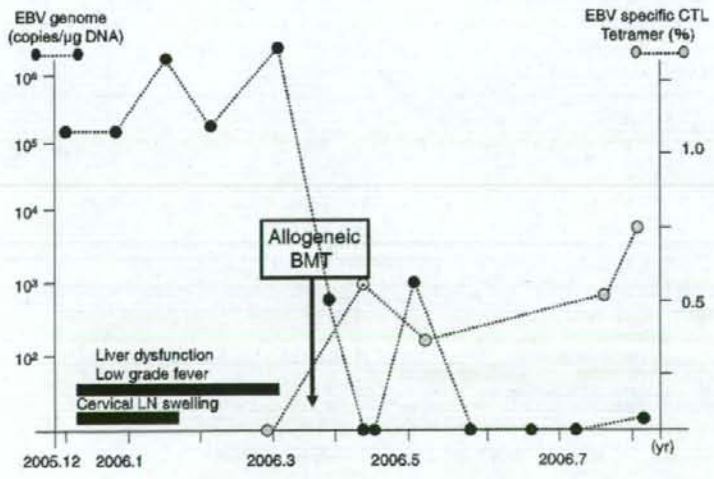

Fig. 1. The clinical course of the patient 1 (case 1) is depicted. EBV-specific CTL activities of the patient 1 before BMT and after BMT (day 21) measured by the tetramer method are shown.

the EBV genome titer gradually decreased as the CTL activity increased (0.65%, day 63). At two months after BMT, the EBV genome titer of the patient was nearly negative (Fig. 1).

Case 2

The patient was a two-yr-old girl who had exhibited a persistent fever of unknown etiology and hepatosplenomegaly. Abnormally high titers of EBV-related antibodies were detected and NK cells in her peripheral blood contained a high EBV genome titer (1.4×10^5 copies/μg DNA). EBV-terminal repeats showed a single band by Southern blotting analysis. Her NK-cell activity was normal. EBV-specific CTL activity was low (0.29%, using the tetramer method). The patient had no family history of similar disease. She was diagnosed as NK-cell-type CAEBV. At onset, pancytopenia, liver dysfunction, high LDH, and hyperferritinemia were detected. A corticosteroid, immunosuppressant (cyclosporin A), and etoposide (VP16) were administered and her symptoms improved. However, one month later, fever and liver dysfunction reappeared. The viral load increased, which was considered to be indicative of a recurrence. After six months, HLA full-matched unrelated BMT was performed. The preconditioning regimen consisted of TBI, CPM, and thiotepa. Bone marrow recovery was rapid, and transplantation-related toxicity was not so severe. Acute GVHD was grade 1 (skin). Her clinical course is depicted in Fig. 2. In this case, fever, liver dysfunction, and hyperferritinemia reappeared and the EBV genome increased one wk before the preconditioning chemotherapy, so recurrence was suspected. These symptoms gradually improved after the start of preconditioning chemotherapy. Complete donor chimerism was established by STR analysis on day 45 after BMT. The EBV genome numbers and EBV-specific CTL levels were measured during her clinical course. High EBV genome titers and low EBV-specific CTL activity were detected before BMT (0.29%). After BMT, the EBV genome titers decreased gradually as the CTL activity increased (0.76%, day 37) (Fig. 2).

Discussion

EBV is a member of the herpes virus family. Most individuals are infected by early adulthood. In healthy carriers, EBV persists in a latent state lifelong in resting memory B cells. Recently, some reports suggested that EBV plays a role in a variety of diseases (1, 16).

CAEBV is characterized by chronic or recurrent infectious mononucleosis-like symptoms that persist for a long time and by an abnormal pattern of antibodies to EBV. High virus load is detected in the peripheral blood of patients with CAEBV. Recently, diagnostic criteria have been proposed (7, 17). Although the pathogenesis and etiology were unclear, it has been reported that the clonal expansion of EBV-infected T or NK cells might be associated with the development of CAEBV (5, 6, 8, 9, 18). However, oligoclonal expansion of EBV-infected lymphocyte has been reported, so it is not clear whether CAEBV is truly a monoclonal disorder or not (10).

Although CAEBV is severe disease that can be fatal if not treated appropriately, standard treatment regimens have not been established. Treatments such as antiviral agents,

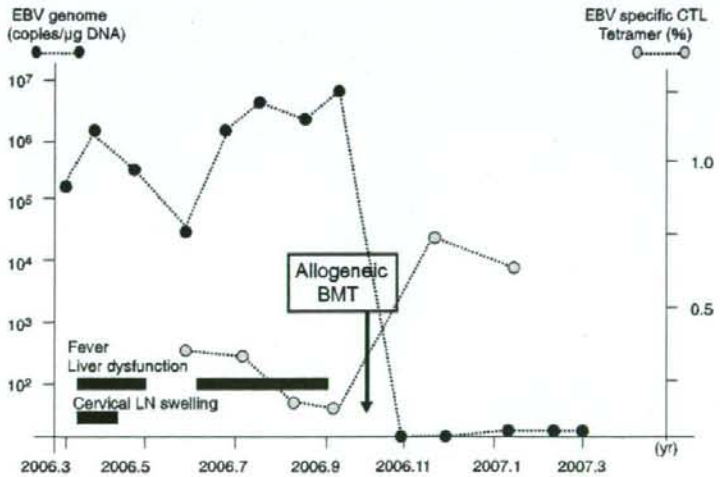

Fig. 2. The clinical course of the patient 2 (case 2) is depicted. EBV-specific CTL activities of the patient 2 before BMT and after BMT (day 26) measured by the tetramer method are shown.

18. Knowles DM. Immunodeficiency-associated lymphoproliferative disorders. Mod Pathol 1999: 12: 200 217.
19. Hoshino Y, Morishima T, Kimura H, Nishikawa K, Tsurumi T, Kuzushima K. Antigen-driven expansion and contraction of CD8+-activated T cells in primary EBV infection. J Immunol 1999: 15: 5735 5740.
20. Callan MFC, Tan L, Annels N. Direct visualization of antigen-specific CD8+ T cells during the primary immune response to Epstein Barr virus in vivo. J Exp Med 1998: 187: 1395 1402.
21. Khanna R, Burrows SR. Role of cytotoxic T lymphocytes in Epstein Barr virus associated diseases. Annu Rev Immunol 1997: 15: 405 431.